

Statistical Validation of a BCS-based Technique for Perfect Electric Conductors Retrieval

L. Poli, G. Oliveri, A. Massa

Abstract

In this report, a statistical analysis of the local shape function multi-task Bayesian compressive sensing technique is proposed. Accuracy and robustness of the technique has been evaluated varying the number and the position of the sparse PEC objects inside investigation domains of different size.

1 TESTS Domain $L = 2.00\lambda$

1.1 Tests Random Objects $l = 0.15\lambda$

GOAL: show the performances of *BCS* when dealing with a sparse scatterer

- Number of Views: V
- Number of Measurements: M
- Number of Cells for the Inversion: N
- Number of Cells for the Direct solver: D
- Side of the investigation domain: L

Test Case Description

Direct solver:

- Square domain divided in $\sqrt{D} \times \sqrt{D}$ cells
- Domain side: $L = 2\lambda$
- $D = 676$ (discretization for the direct solver: $< \lambda/10$)

Investigation domain:

- Square domain divided in $\sqrt{N} \times \sqrt{N}$ cells
- $L = 2\lambda$
- $2ka = 2 \times \frac{2\pi}{\lambda} \times \frac{L\sqrt{2}}{2} = 17.77$
- $\#DOF = \frac{(2ka)^2}{2} = \frac{(2 \times \frac{2\pi}{\lambda} \times \frac{L\sqrt{2}}{2})^2}{2} \approx 162$
- N scelto in modo da essere vicino a $\#DOF$: $N = 169$ (13×13)

Measurement domain:

- Measurement points taken on a circle of radius $\rho = 2\lambda$
- Full-aspect measurements
- $M \approx 2ka \rightarrow M = 18$

Sources:

- Plane waves
- $V \approx 2ka \rightarrow V = 18$
- Amplitude: $A = 1$
- Frequency: 300 MHz ($\lambda = 1$)

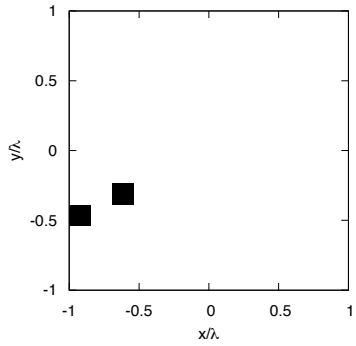
PEC Objects:

- Two square cylinders of side $\frac{2}{13}\lambda \cong 0.15\lambda$
- S sparse square cylinders of side $\frac{2}{13}\lambda \cong 0.15\lambda$ ($S \in \{1, 2, 3, 4, 5, 6, 7, 8\}$). In order to get a statistical validation, for each value of S the simulation has been repeat for 20 times, changing the distribution of the objects inside the investigation domain

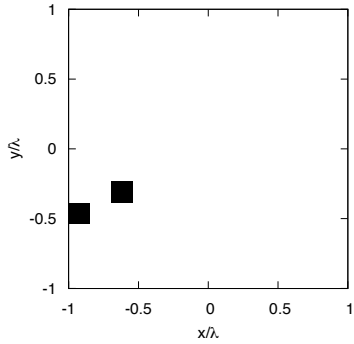
MT-BCS-based technique parameters:

- Gamma prior on noise variance parameter: $a = 5 \times 10^{-2}$
- Gamma prior on noise variance parameter: $b = 5 \times 10^{-2}$
- Convergenze parameter: $\tau = 1.0 \times 10^{-8}$
- Threshold: $\eta = 0.27$

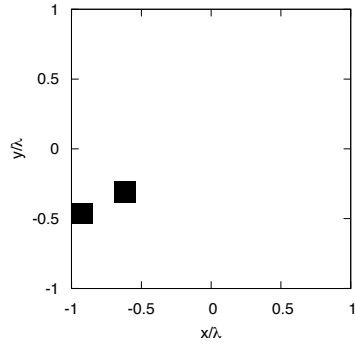
Reconstruction Profiles: $S = 2$ Sparse Cylinders - Best Case



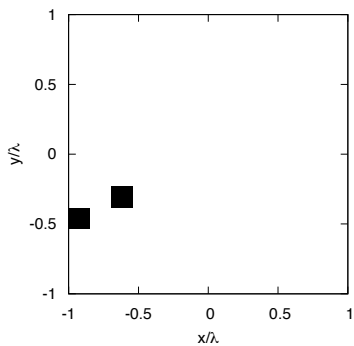
(a)



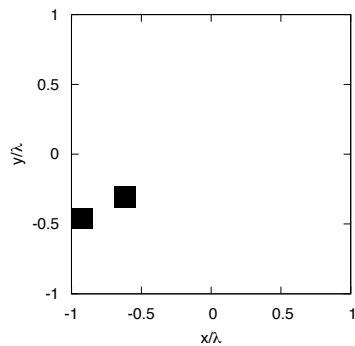
(b)



(c)



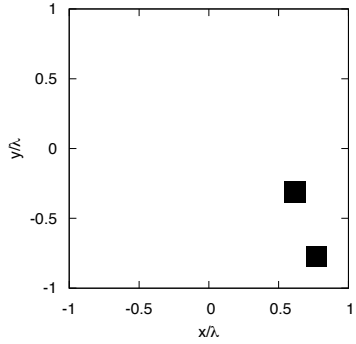
(d)



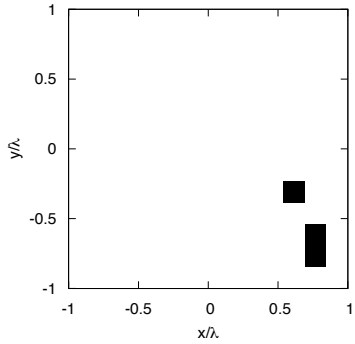
(e)

Figure 1. Actual object (a) and MT-BCS reconstructed object for $SNR = 50$ [dB] (b), $SNR = 30$ [dB] (c), $SNR = 20$ [dB] (d) and $SNR = 10$ [dB] (e).

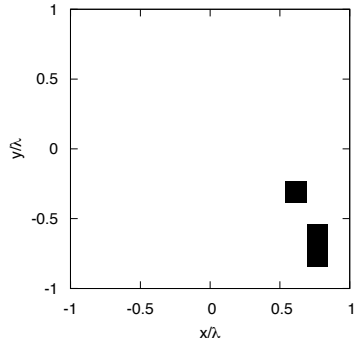
Reconstruction Profiles: $S = 2$ Sparse Cylinders - Worst Case



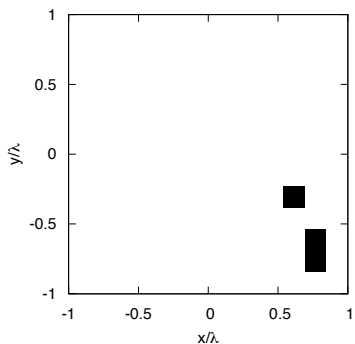
(a)



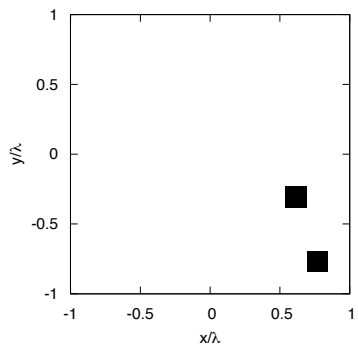
(b)



(c)



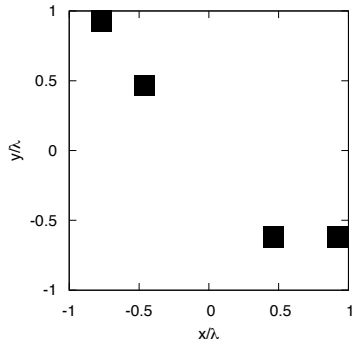
(d)



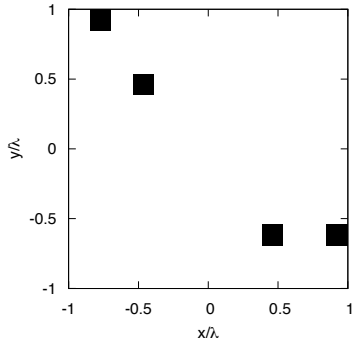
(e)

Figure 2. Actual object (a) and MT-BCS reconstructed object for $SNR = 50$ [dB] (b), $SNR = 30$ [dB] (c), $SNR = 20$ [dB] (d) and $SNR = 10$ [dB] (e).

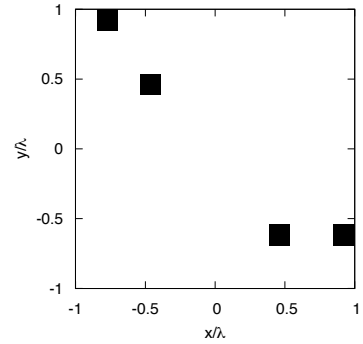
Reconstruction Profiles: $S = 4$ Sparse Cylinders - Best Case



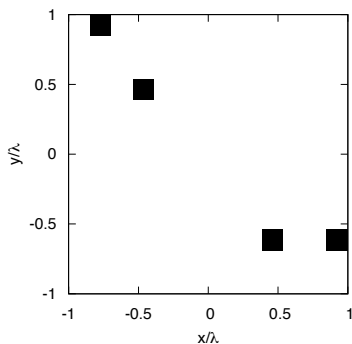
(a)



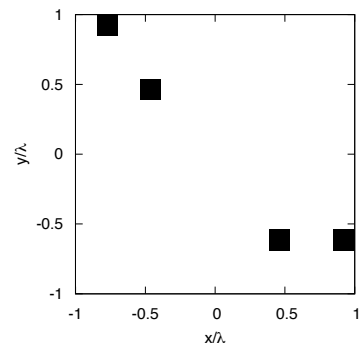
(b)



(c)



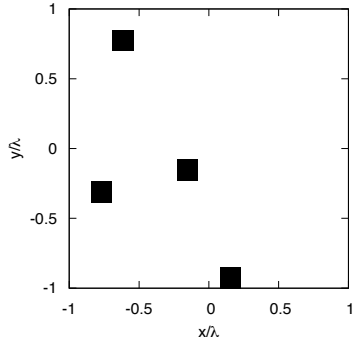
(d)



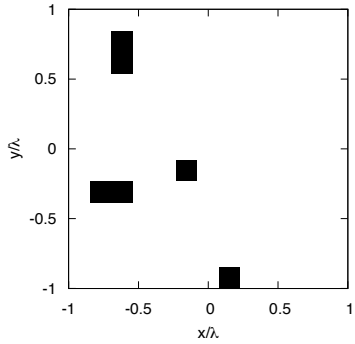
(e)

Figure 3. Actual object (a) and MT-BCS reconstructed object for $SNR = 50$ [dB] (b), $SNR = 30$ [dB] (c), $SNR = 20$ [dB] (d) and $SNR = 10$ [dB] (e).

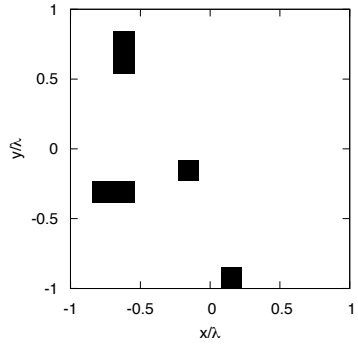
Reconstruction Profiles: $S = 4$ Sparse Cylinders - Worst Case



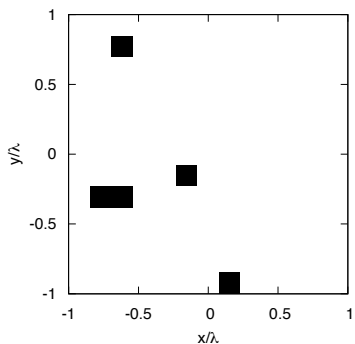
(a)



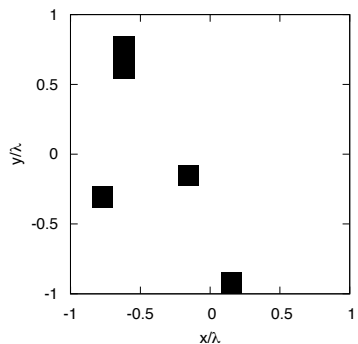
(b)



(c)



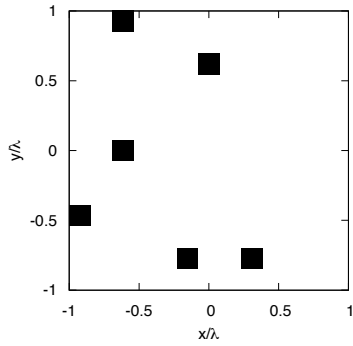
(d)



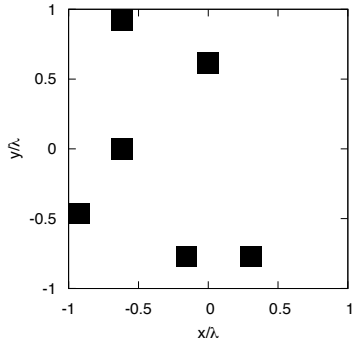
(e)

Figure 4. Actual object (a) and MT-BCS reconstructed object for $SNR = 50$ [dB] (b), $SNR = 30$ [dB] (c), $SNR = 20$ [dB] (d) and $SNR = 10$ [dB] (e).

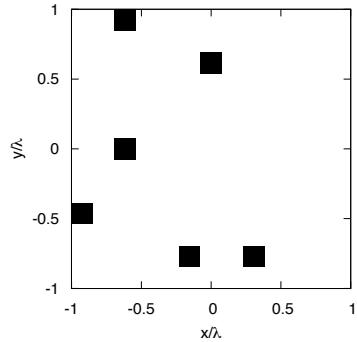
Reconstruction Profiles: $S = 6$ Sparse Cylinders - Best Case



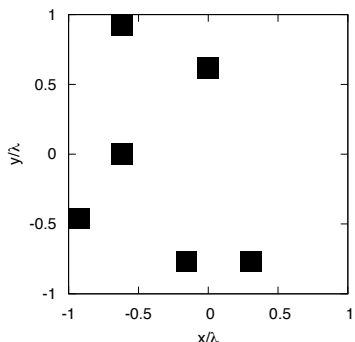
(a)



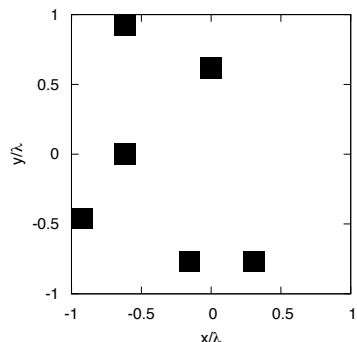
(b)



(c)



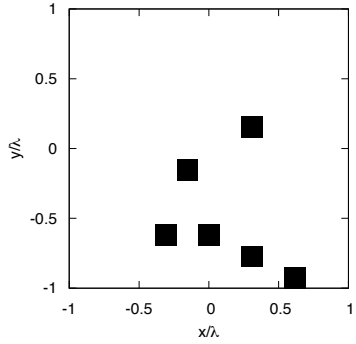
(d)



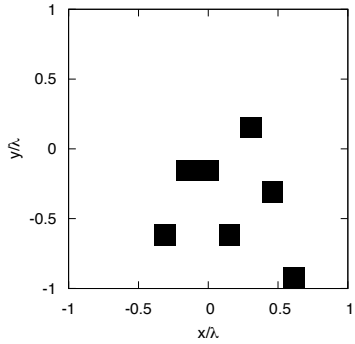
(e)

Figure 5. Actual object (a) and MT-BCS reconstructed object for $SNR = 50$ [dB] (b), $SNR = 30$ [dB] (c), $SNR = 20$ [dB] (d) and $SNR = 10$ [dB] (e).

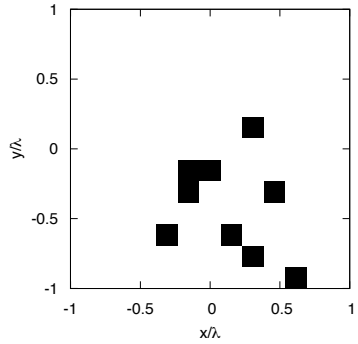
Reconstruction Profiles: $S = 6$ Sparse Cylinders - Worst Case



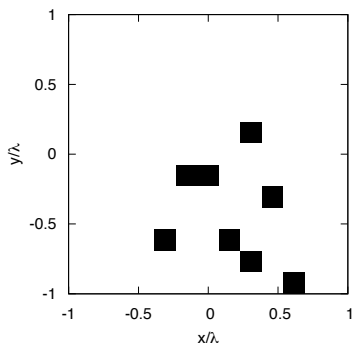
(a)



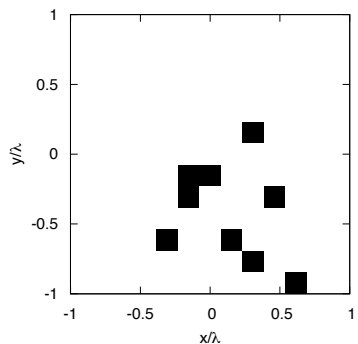
(b)



(c)



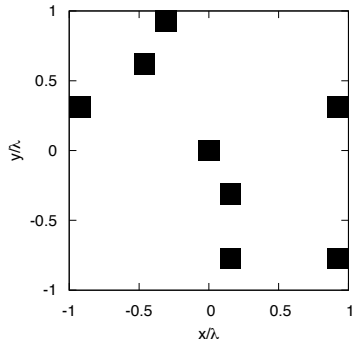
(d)



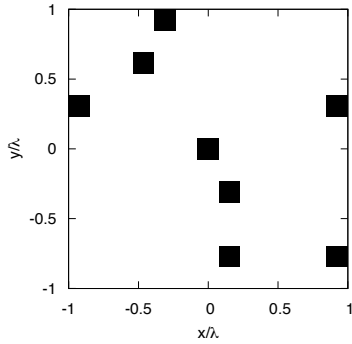
(e)

Figure 6. Actual object (a) and MT-BCS reconstructed object for $SNR = 50$ [dB] (b), $SNR = 30$ [dB] (c), $SNR = 20$ [dB] (d) and $SNR = 10$ [dB] (e).

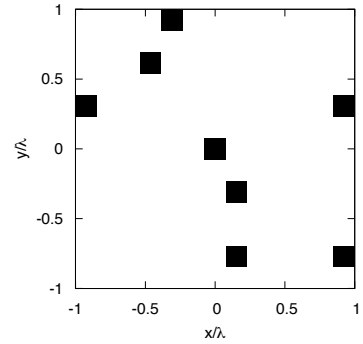
Reconstruction Profiles: $S = 8$ Sparse Cylinders - Best Case



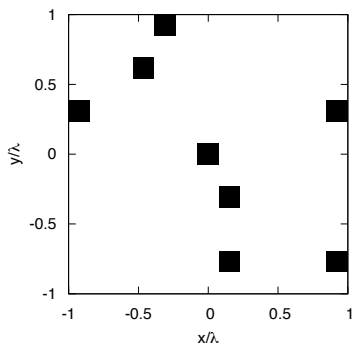
(a)



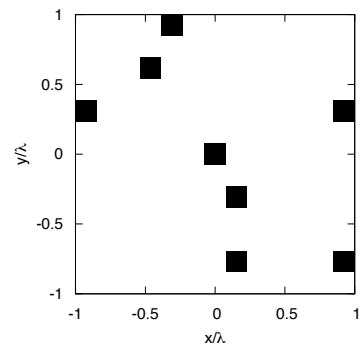
(b)



(c)



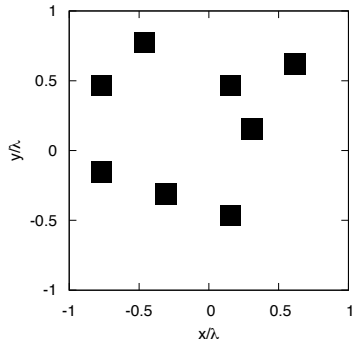
(d)



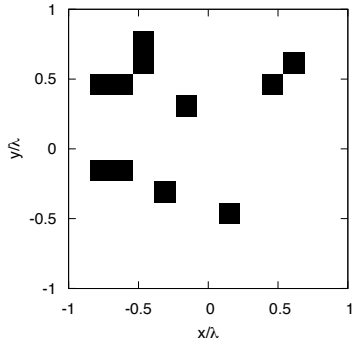
(e)

Figure 7. Actual object (a) and MT-BCS reconstructed object for $SNR = 50$ [dB] (b), $SNR = 30$ [dB] (c), $SNR = 20$ [dB] (d) and $SNR = 10$ [dB] (e).

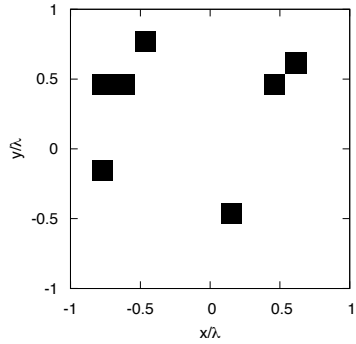
Reconstruction Profiles: $S = 8$ Sparse Cylinders - Worst Case



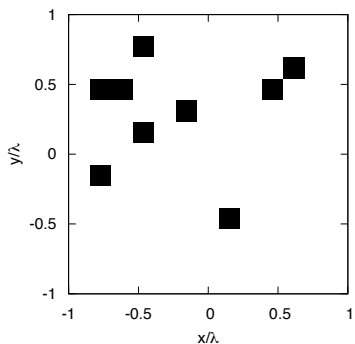
(a)



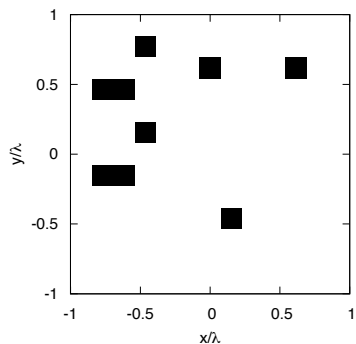
(b)



(c)



(d)



(e)

Figure 8. Actual object (a) and MT-BCS reconstructed object for $SNR = 50$ [dB] (b), $SNR = 30$ [dB] (c), $SNR = 20$ [dB] (d) and $SNR = 10$ [dB] (e).

Resume: Domain $L = 2.0\lambda$ - Statistical Analysis - Error Figures

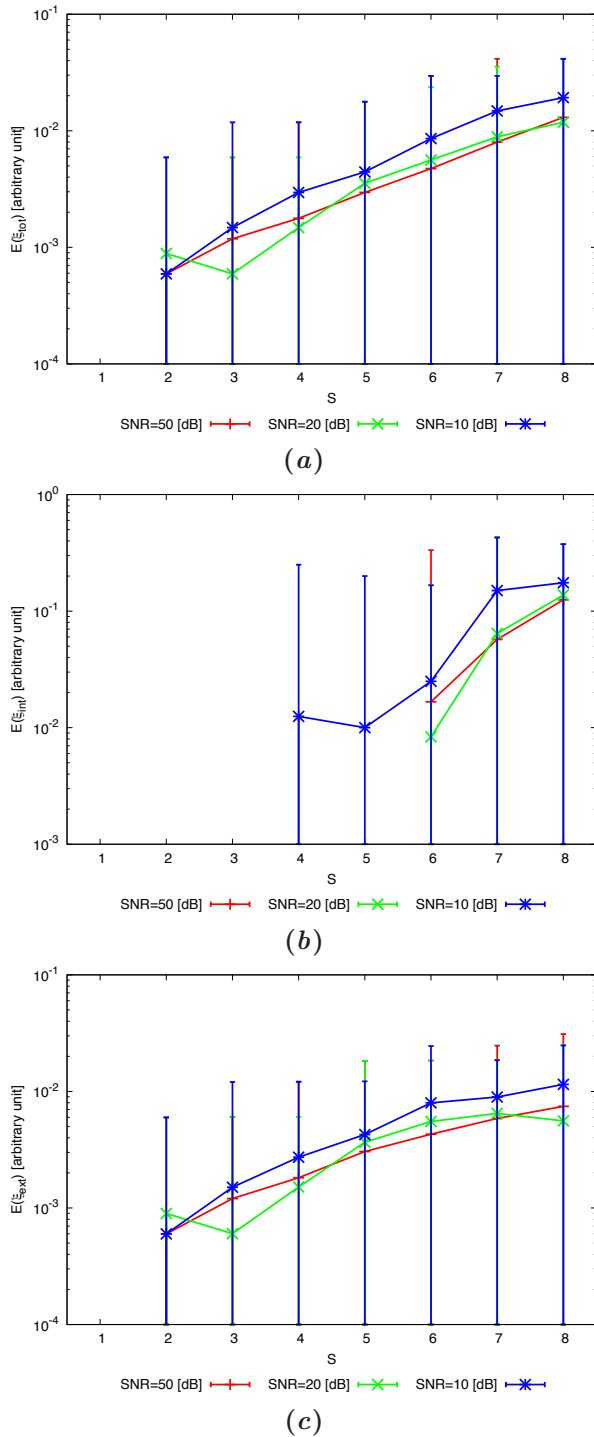


Figure 9. Statistical Analysis - Behavior of mean, maximum and minimum of the error figures as a function of S of the total error ξ_{tot} (a), internal error ξ_{int} (b) and external error ξ_{ext} (c).

2 TESTS Domain $L = 3.00\lambda$

2.1 Tests Random Objects $l = 0.16\lambda$

GOAL: show the performances of BCS when dealing with a sparse scatterer

- Number of Views: V
- Number of Measurements: M
- Number of Cells for the Inversion: N
- Number of Cells for the Direct solver: D
- Side of the investigation domain: L

Test Case Description

Direct solver:

- Square domain divided in $\sqrt{D} \times \sqrt{D}$ cells
- Domain side: $L = 3\lambda$
- $D = 1296$ (discretization for the direct solver: $< \lambda/10$)

Investigation domain:

- Square domain divided in $\sqrt{N} \times \sqrt{N}$ cells
- $L = 3\lambda$
- $2ka = 2 \times \frac{2\pi}{\lambda} \times \frac{L\sqrt{2}}{2} = 26.66$
- $\#DOF = \frac{(2ka)^2}{2} = \frac{(2 \times \frac{2\pi}{\lambda} \times \frac{L\sqrt{2}}{2})^2}{2} \approx 364.5$
- N scelto in modo da essere vicino a $\#DOF$: $N = 324$ (18×18)

Measurement domain:

- Measurement points taken on a circle of radius $\rho = 3\lambda$
- Full-aspect measurements
- $M \approx 2ka \rightarrow M = 27$

Sources:

- Plane waves
- $V \approx 2ka \rightarrow V = 27$
- Amplitude: $A = 1$
- Frequency: 300 MHz ($\lambda = 1$)

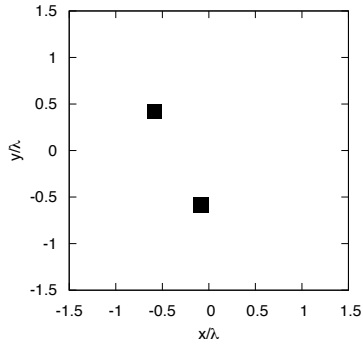
PEC Objects:

- Two square cylinders of side $\frac{\lambda}{6} \cong 0.16\lambda$
- S sparse square cylinders of side $\frac{\lambda}{6} \cong 0.16\lambda$ ($S \in \{1, 2, 3, 4, 5, 6\}$). In order to get a statistical validation, for each value of S the simulation has been repeat for 20 times, changing the distribution of the objects inside the investigation domain

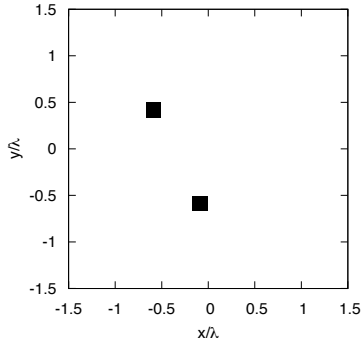
MT-BCS-based technique parameters:

- Gamma prior on noise variance parameter: $a = 5 \times 10^{-2}$
- Gamma prior on noise variance parameter: $b = 5 \times 10^{-2}$
- Convergenze parameter: $\tau = 1.0 \times 10^{-8}$
- Threshold: $\eta = 0.27$

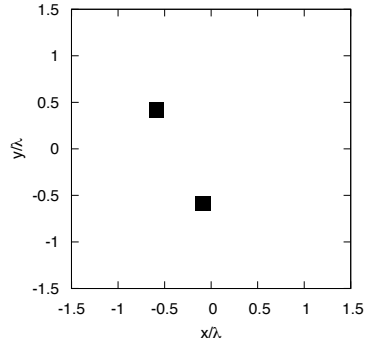
Reconstruction Profiles: $S = 2$ Sparse Cylinders - Best Case



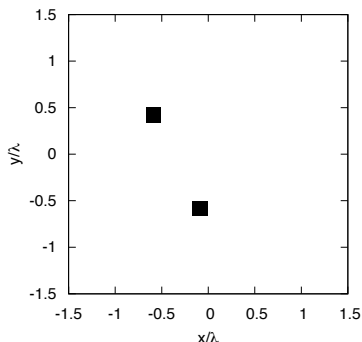
(a)



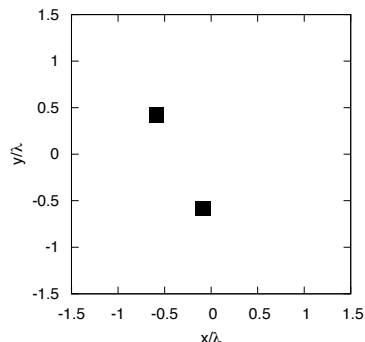
(b)



(c)



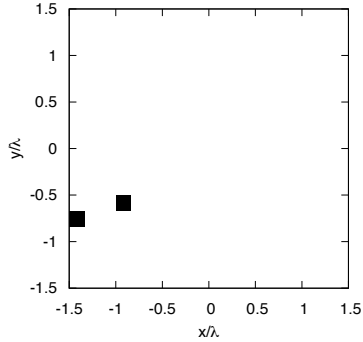
(d)



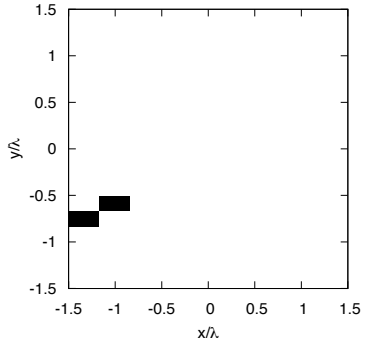
(e)

Figure 10. Actual object (a) and MT-BCS reconstructed object for $SNR = 50$ [dB] (b), $SNR = 30$ [dB] (c), $SNR = 20$ [dB] (d) and $SNR = 10$ [dB] (e).

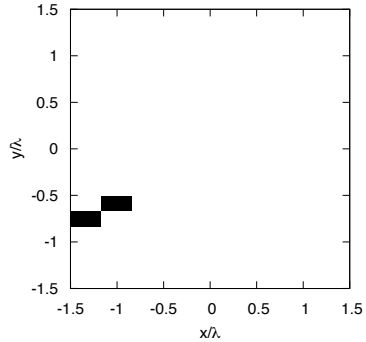
Reconstruction Profiles: $S = 2$ Sparse Cylinders - Worst Case



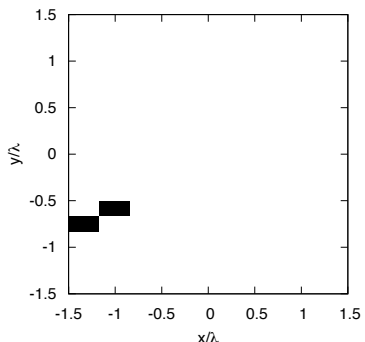
(a)



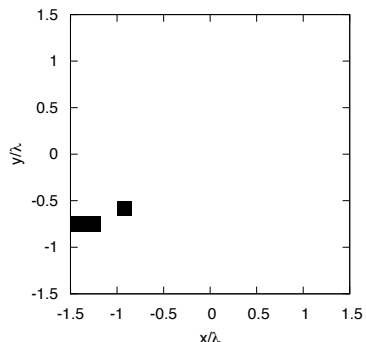
(b)



(c)



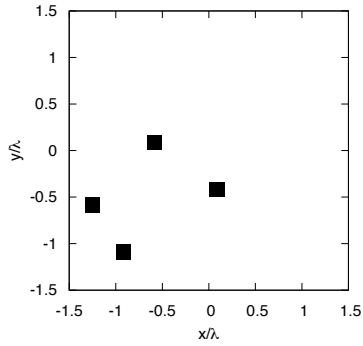
(d)



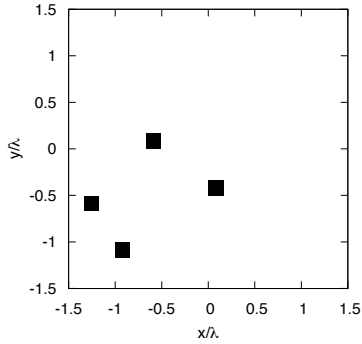
(e)

Figure 11. Actual object (a) and MT-BCS reconstructed object for $SNR = 50$ [dB] (b), $SNR = 30$ [dB] (c), $SNR = 20$ [dB] (d) and $SNR = 10$ [dB] (e).

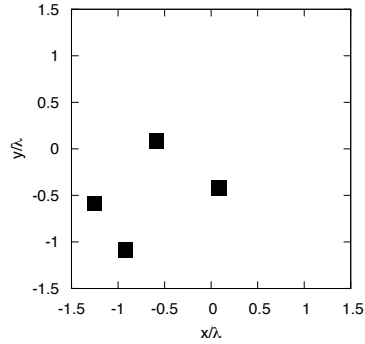
Reconstruction Profiles: $S = 4$ Sparse Cylinders - Best Case



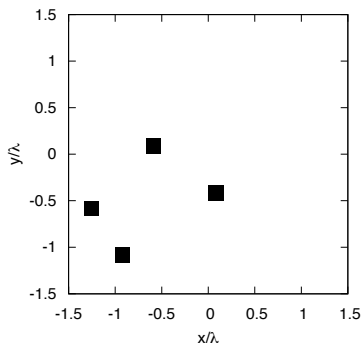
(a)



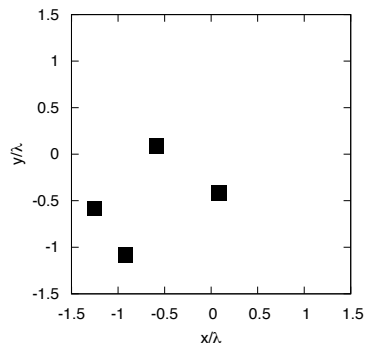
(b)



(c)



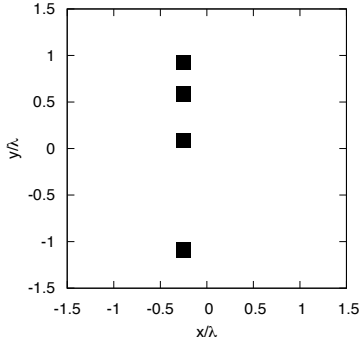
(d)



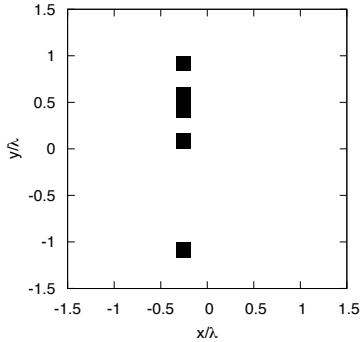
(e)

Figure 12. Actual object (a) and MT-BCS reconstructed object for $SNR = 50$ [dB] (b), $SNR = 30$ [dB] (c), $SNR = 20$ [dB] (d) and $SNR = 10$ [dB] (e).

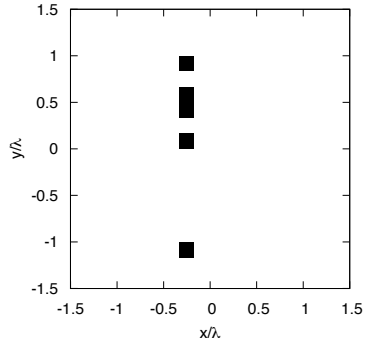
Reconstruction Profiles: $S = 4$ Sparse Cylinders - Worst Case



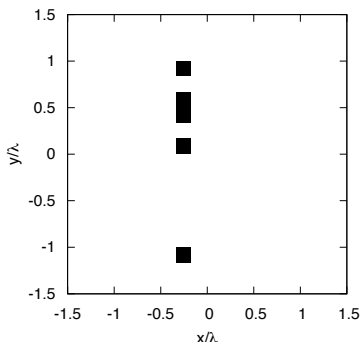
(a)



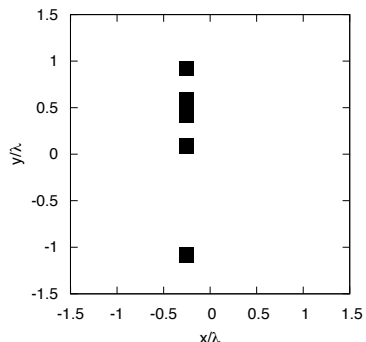
(b)



(c)



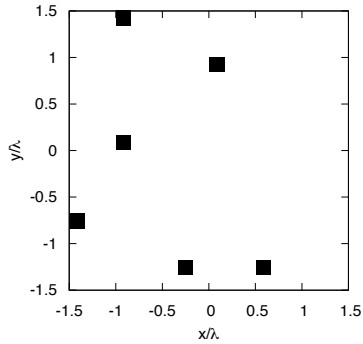
(d)



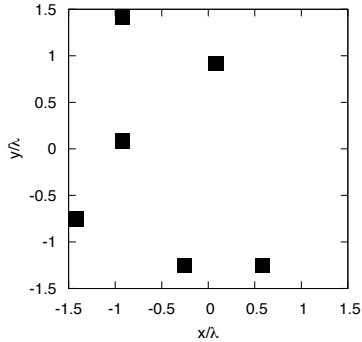
(e)

Figure 13. Actual object (a) and MT-BCS reconstructed object for $SNR = 50$ [dB] (b), $SNR = 30$ [dB] (c), $SNR = 20$ [dB] (d) and $SNR = 10$ [dB] (e).

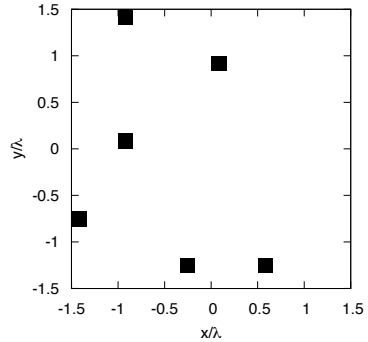
Reconstruction Profiles: $S = 6$ Sparse Cylinders - Best Case



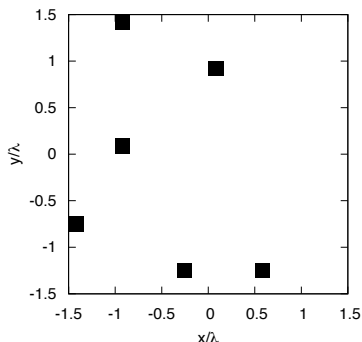
(a)



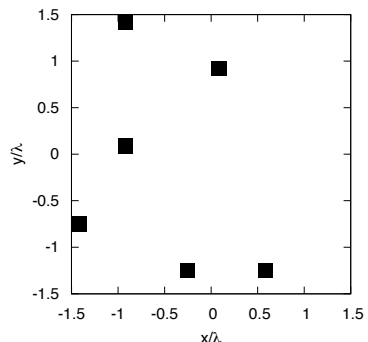
(b)



(c)



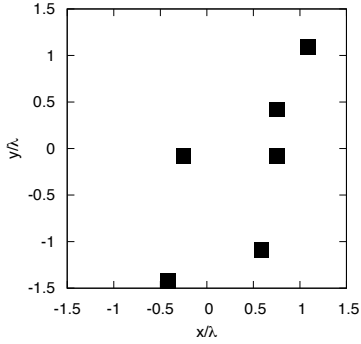
(d)



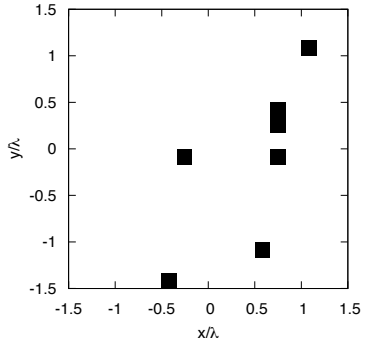
(e)

Figure 14. Actual object (a) and MT-BCS reconstructed object for $SNR = 50$ [dB] (b), $SNR = 30$ [dB] (c), $SNR = 20$ [dB] (d) and $SNR = 10$ [dB] (e).

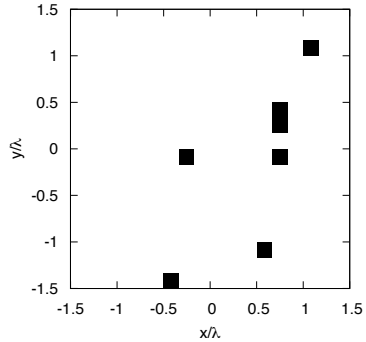
Reconstruction Profiles: $S = 6$ Sparse Cylinders - Worst Case



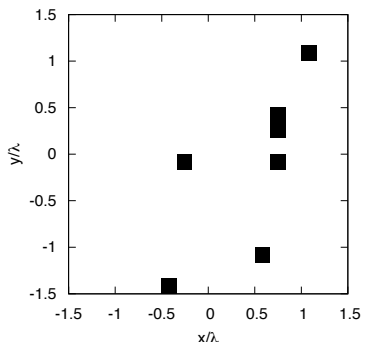
(a)



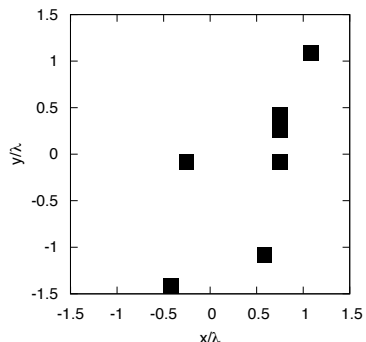
(b)



(c)



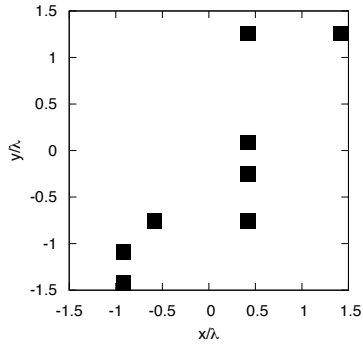
(d)



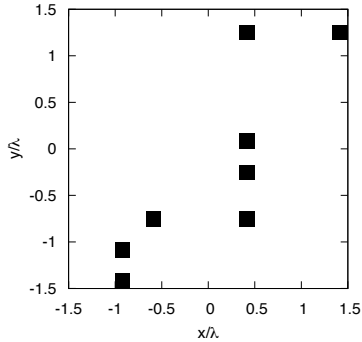
(e)

Figure 15. Actual object (a) and MT-BCS reconstructed object for $SNR = 50$ [dB] (b), $SNR = 30$ [dB] (c), $SNR = 20$ [dB] (d) and $SNR = 10$ [dB] (e).

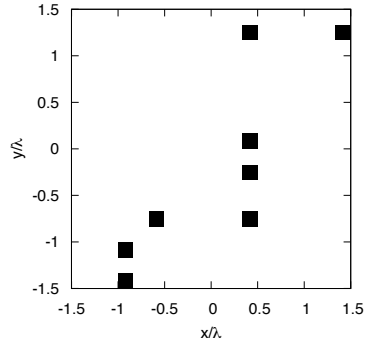
Reconstruction Profiles: $S = 8$ Sparse Cylinders - Best Case



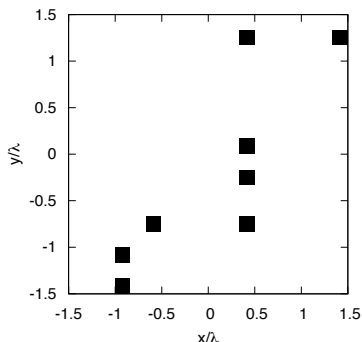
(a)



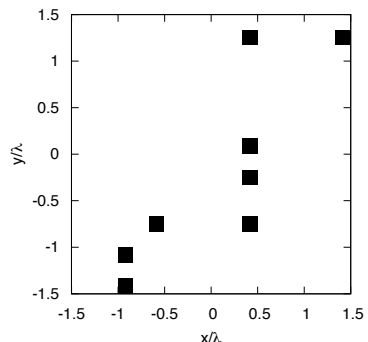
(b)



(c)



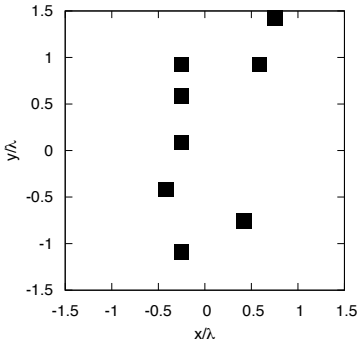
(d)



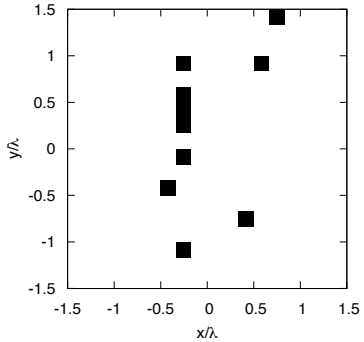
(e)

Figure 16. Actual object (a) and MT-BCS reconstructed object for $SNR = 50$ [dB] (b), $SNR = 30$ [dB] (c), $SNR = 20$ [dB] (d) and $SNR = 10$ [dB] (e).

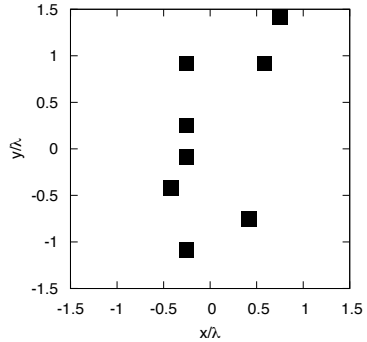
Reconstruction Profiles: $S = 8$ Sparse Cylinders - Worst Case



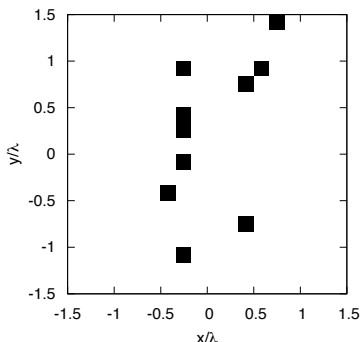
(a)



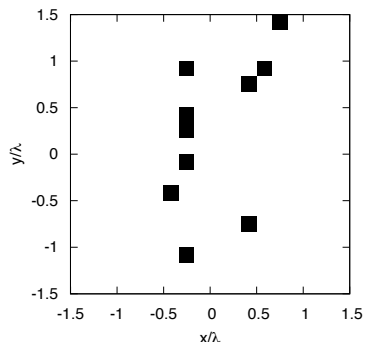
(b)



(c)



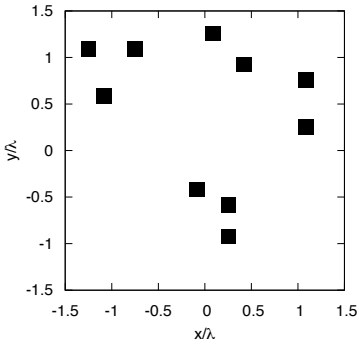
(d)



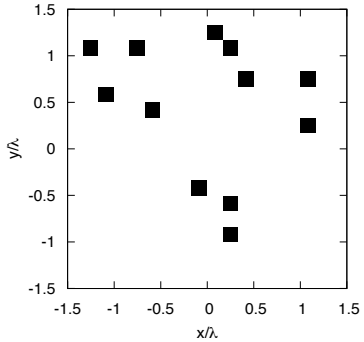
(e)

Figure 17. Actual object (a) and MT-BCS reconstructed object for $SNR = 50$ [dB] (b), $SNR = 30$ [dB] (c), $SNR = 20$ [dB] (d) and $SNR = 10$ [dB] (e).

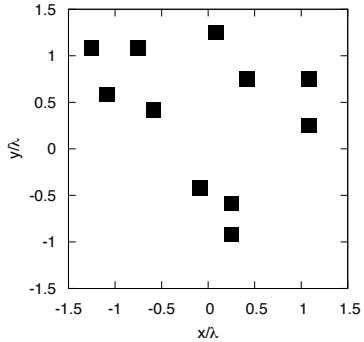
Reconstruction Profiles: $S = 10$ Sparse Cylinders - Best Case



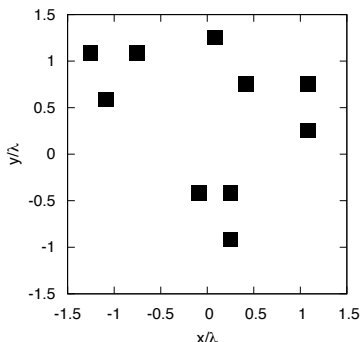
(a)



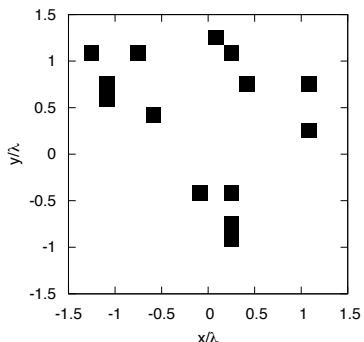
(b)



(c)



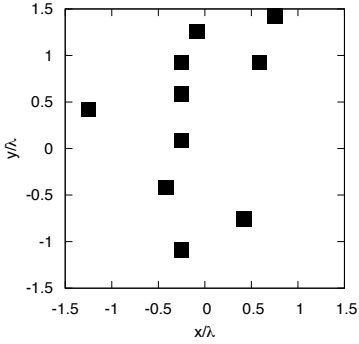
(d)



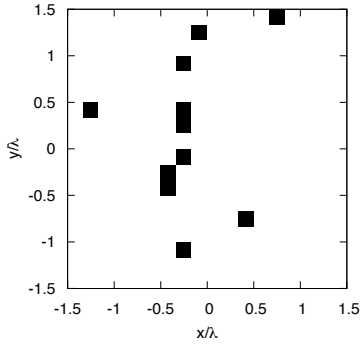
(e)

Figure 18. Actual object (a) and MT-BCS reconstructed object for $SNR = 50$ [dB] (b), $SNR = 30$ [dB] (c), $SNR = 20$ [dB] (d) and $SNR = 10$ [dB] (e).

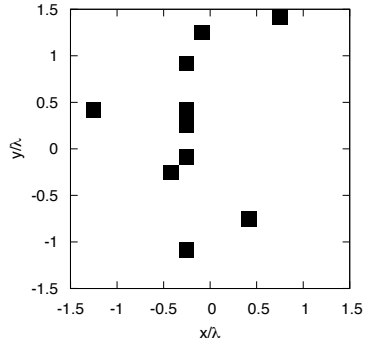
Reconstruction Profiles: $S = 10$ Sparse Cylinders - Worst Case



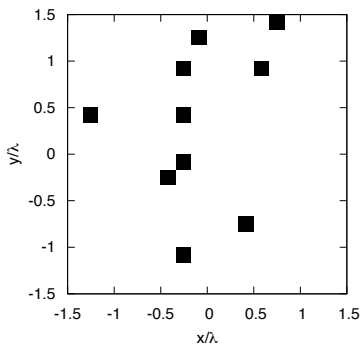
(a)



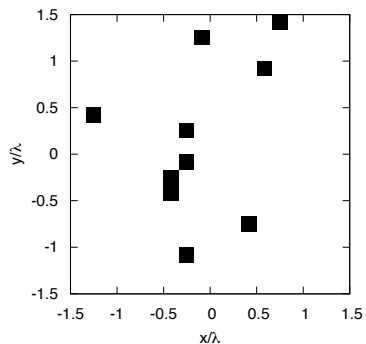
(b)



(c)



(d)



(e)

Figure 19. Actual object (a) and MT-BCS reconstructed object for $SNR = 50$ [dB] (b), $SNR = 30$ [dB] (c), $SNR = 20$ [dB] (d) and $SNR = 10$ [dB] (e).

Resume: Domain $L = 3.0\lambda$ - Statistical Analysis - Error Figures

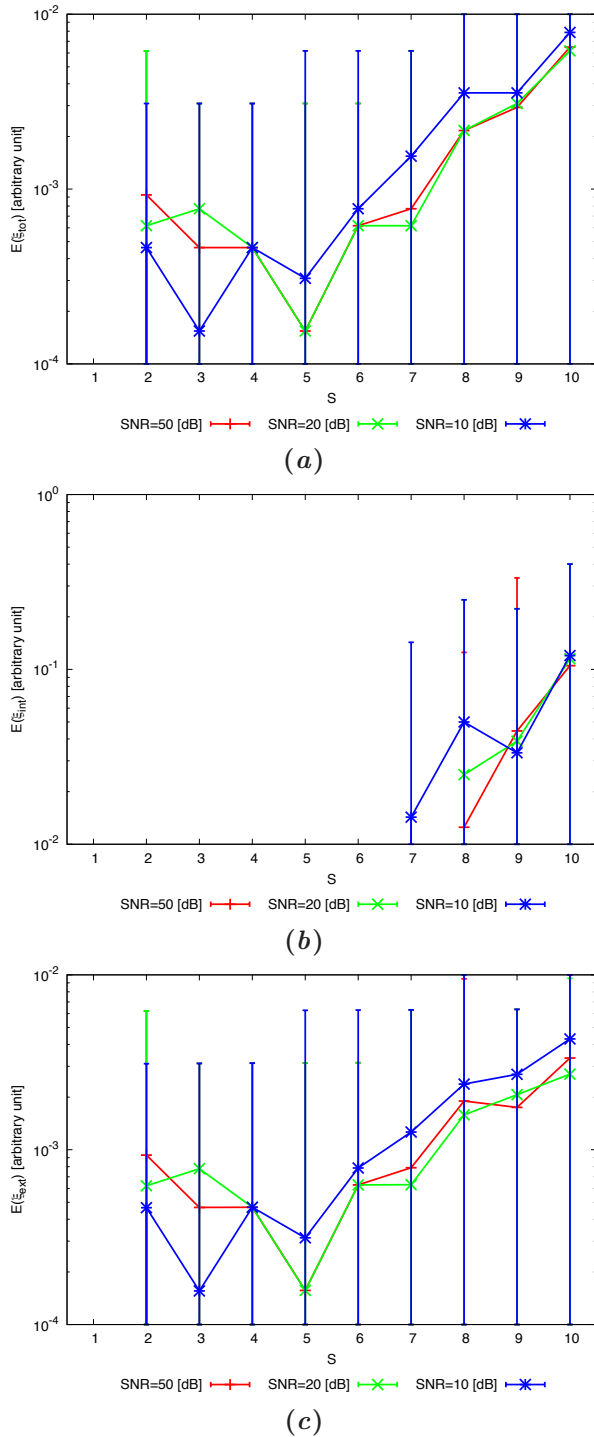


Figure 20. *Statistical Analysis - Behavior of mean, maximum and minimum of the error figures as a function of S of the total error ξ_{tot} (a), internal error ξ_{int} (b) and external error ξ_{ext} (c).*

2.2 Tests Random Objects $l = 0.33\lambda$

GOAL: show the performances of *BCS* when dealing with a sparse scatterer

- Number of Views: V
- Number of Measurements: M
- Number of Cells for the Inversion: N
- Number of Cells for the Direct solver: D
- Side of the investigation domain: L

Test Case Description

Direct solver:

- Square domain divided in $\sqrt{D} \times \sqrt{D}$ cells
- Domain side: $L = 3\lambda$
- $D = 1296$ (discretization for the direct solver: $< \lambda/10$)

Investigation domain:

- Square domain divided in $\sqrt{N} \times \sqrt{N}$ cells
- $L = 3\lambda$
- $2ka = 2 \times \frac{2\pi}{\lambda} \times \frac{L\sqrt{2}}{2} = 26.66$
- $\#DOF = \frac{(2ka)^2}{2} = \frac{(2 \times \frac{2\pi}{\lambda} \times \frac{L\sqrt{2}}{2})^2}{2} \approx 364.5$
- N scelto in modo da essere vicino a $\#DOF$: $N = 324$ (18×18)

Measurement domain:

- Measurement points taken on a circle of radius $\rho = 3\lambda$
- Full-aspect measurements
- $M \approx 2ka \rightarrow M = 27$

Sources:

- Plane waves
- $V \approx 2ka \rightarrow V = 27$
- Amplitude: $A = 1$
- Frequency: 300 MHz ($\lambda = 1$)

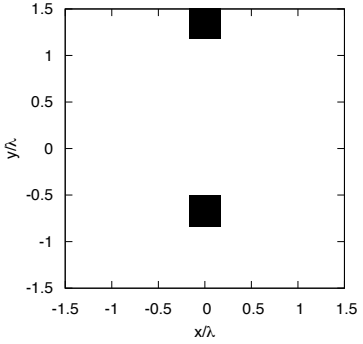
PEC Objects:

- Two square cylinders of side $\frac{\lambda}{3} \cong 0.33\lambda$
- S sparse square cylinders of side $\frac{\lambda}{3} \cong 0.33\lambda$ ($S \in \{1, 2, 3, 4, 5\}$). In order to get a statistical validation, for each value of S the simulation has been repeat for 20 times, changing the distribution of the objects inside the investigation domain

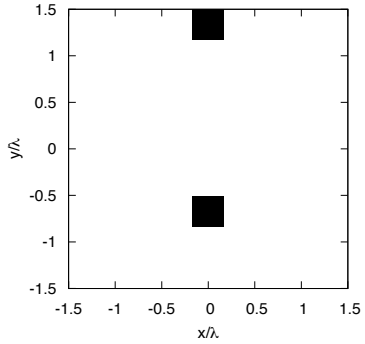
MT-BCS-based technique parameters:

- Gamma prior on noise variance parameter: $a = 5 \times 10^{-2}$
- Gamma prior on noise variance parameter: $b = 5 \times 10^{-2}$
- Convergenze parameter: $\tau = 1.0 \times 10^{-8}$
- Threshold: $\eta = 0.27$

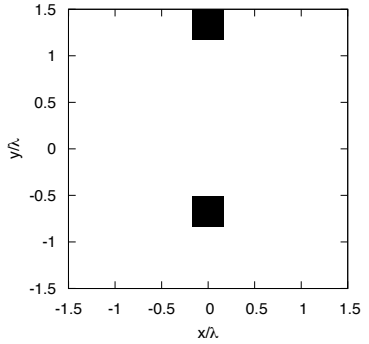
Reconstruction Profiles: $S = 2$ Sparse Cylinders $l = 0.33\lambda$ - Best Case



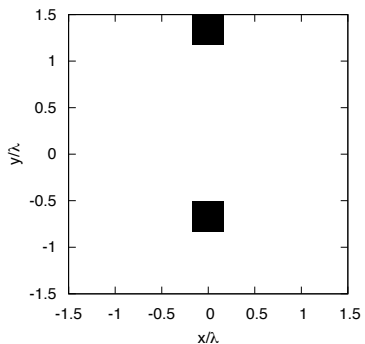
(a)



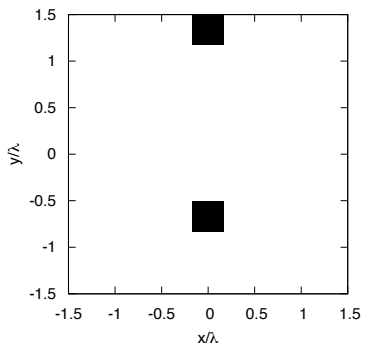
(b)



(c)



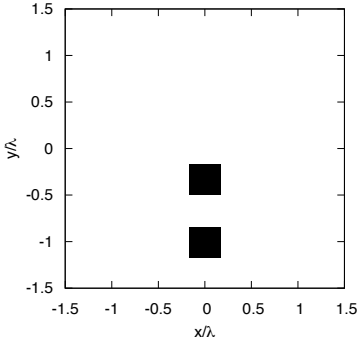
(d)



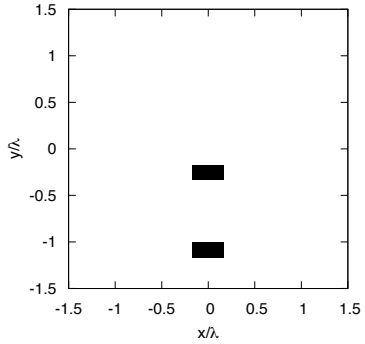
(e)

Figure 21. Actual object (a) and MT-BCS reconstructed object for $SNR = 50$ [dB] (b), $SNR = 30$ [dB] (c), $SNR = 20$ [dB] (d) and $SNR = 10$ [dB] (e).

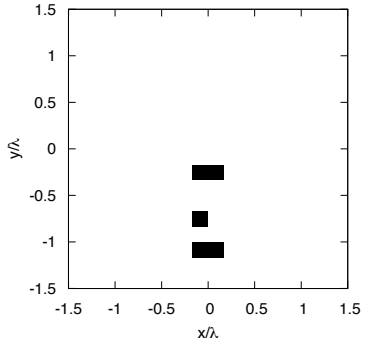
Reconstruction Profiles: $S = 2$ Sparse Cylinders $l = 0.33\lambda$ - Worst Case



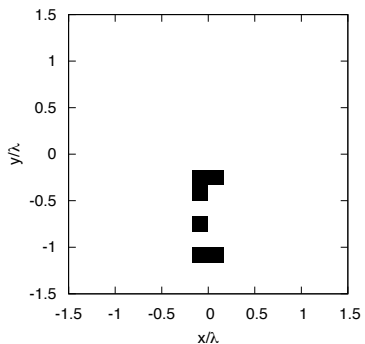
(a)



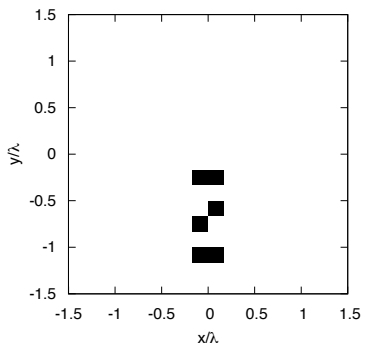
(b)



(c)



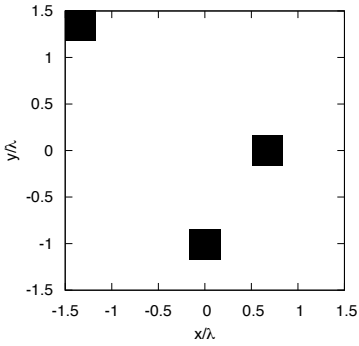
(d)



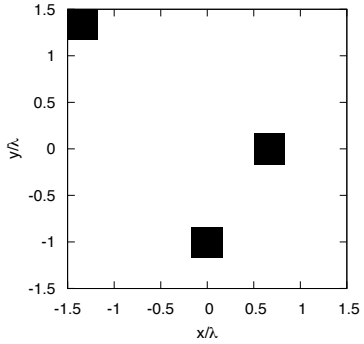
(e)

Figure 22. Actual object (a) and MT-BCS reconstructed object for $SNR = 50$ [dB] (b), $SNR = 30$ [dB] (c), $SNR = 20$ [dB] (d) and $SNR = 10$ [dB] (e).

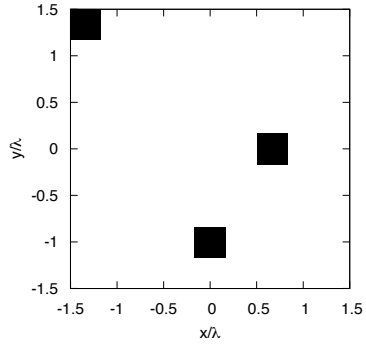
Reconstruction Profiles: $S = 3$ Sparse Cylinders $l = 0.33\lambda$ - Best Case



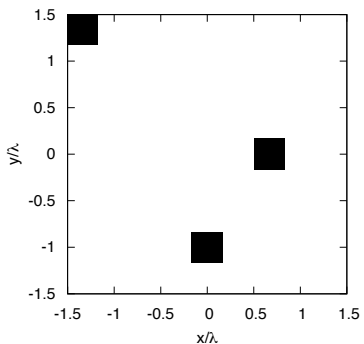
(a)



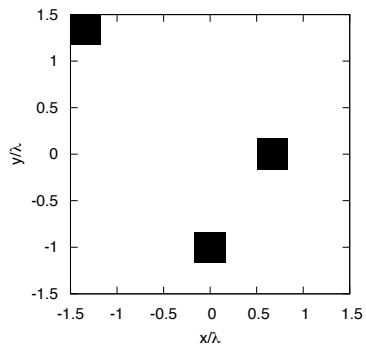
(b)



(c)



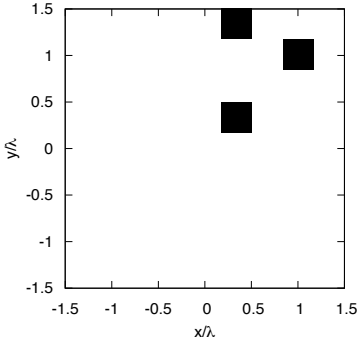
(d)



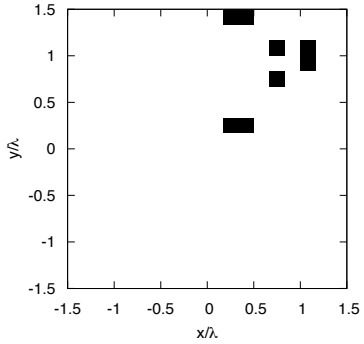
(e)

Figure 23. Actual object (a) and MT-BCS reconstructed object for $SNR = 50$ [dB] (b), $SNR = 30$ [dB] (c), $SNR = 20$ [dB] (d) and $SNR = 10$ [dB] (e).

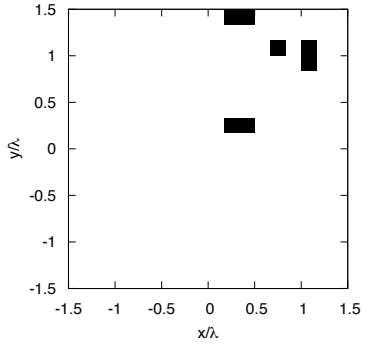
Reconstruction Profiles: $S = 3$ Sparse Cylinders $l = 0.33\lambda$ - Worst Case



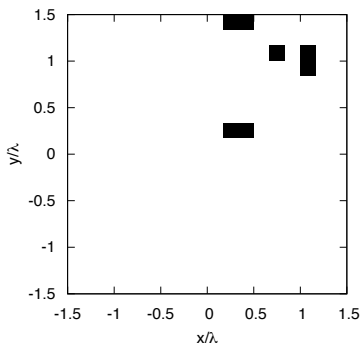
(a)



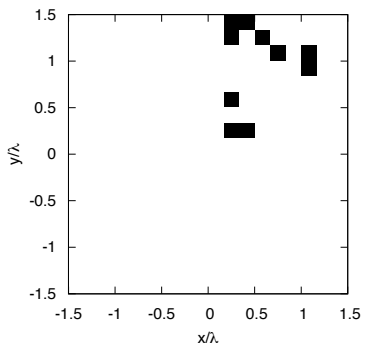
(b)



(c)



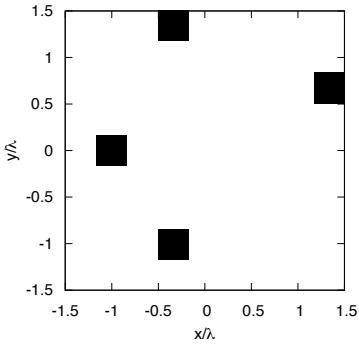
(d)



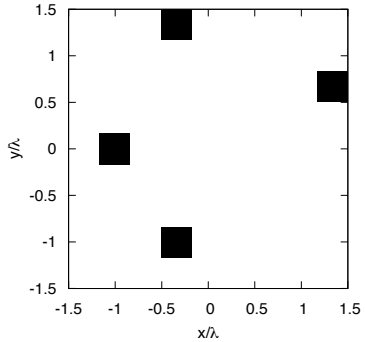
(e)

Figure 24. Actual object (a) and MT-BCS reconstructed object for $SNR = 50$ [dB] (b), $SNR = 30$ [dB] (c), $SNR = 20$ [dB] (d) and $SNR = 10$ [dB] (e).

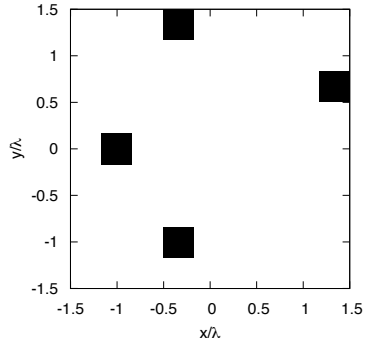
Reconstruction Profiles: $S = 4$ Sparse Cylinders $l = 0.33\lambda$ - Best Case



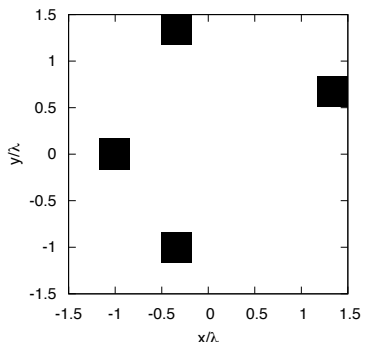
(a)



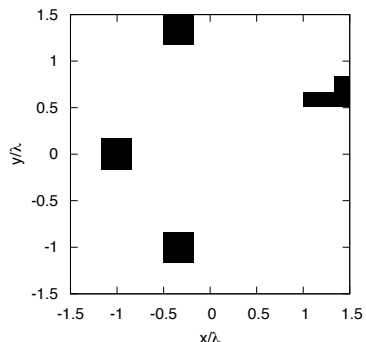
(b)



(c)



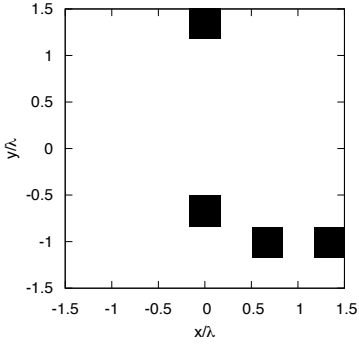
(d)



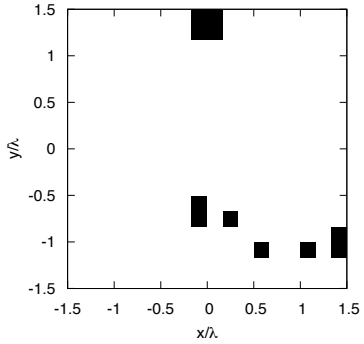
(e)

Figure 25. Actual object (a) and MT-BCS reconstructed object for $SNR = 50$ [dB] (b), $SNR = 30$ [dB] (c), $SNR = 20$ [dB] (d) and $SNR = 10$ [dB] (e).

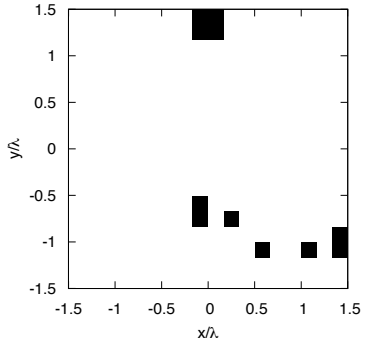
Reconstruction Profiles: $S = 4$ Sparse Cylinders $l = 0.33\lambda$ - Worst Case



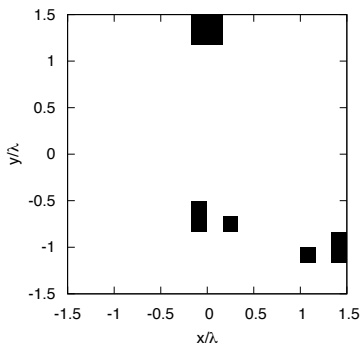
(a)



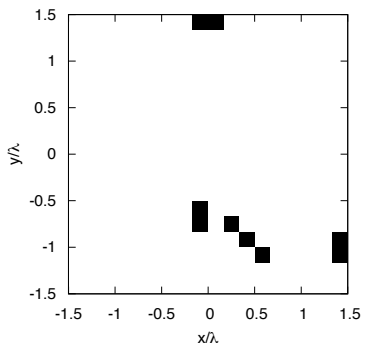
(b)



(c)



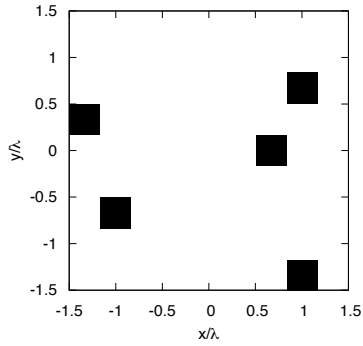
(d)



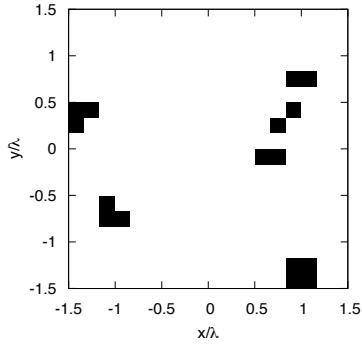
(e)

Figure 26. Actual object (a) and MT-BCS reconstructed object for $SNR = 50$ [dB] (b), $SNR = 30$ [dB] (c), $SNR = 20$ [dB] (d) and $SNR = 10$ [dB] (e).

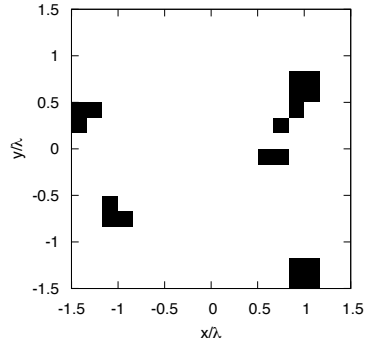
Reconstruction Profiles: $S = 5$ Sparse Cylinders $l = 0.33\lambda$ - Best Case



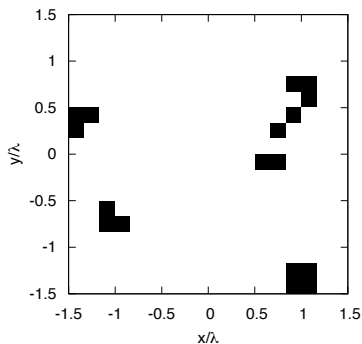
(a)



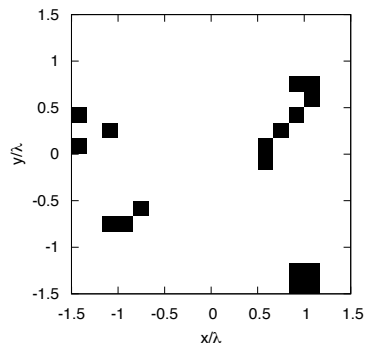
(b)



(c)



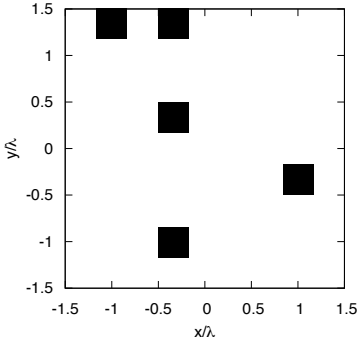
(d)



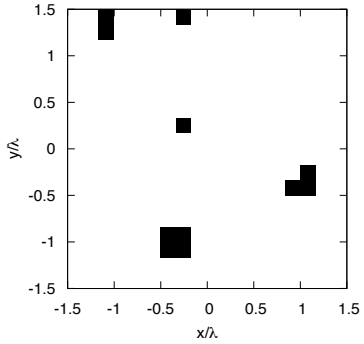
(e)

Figure 27. Actual object (a) and MT-BCS reconstructed object for $SNR = 50$ [dB] (b), $SNR = 30$ [dB] (c), $SNR = 20$ [dB] (d) and $SNR = 10$ [dB] (e).

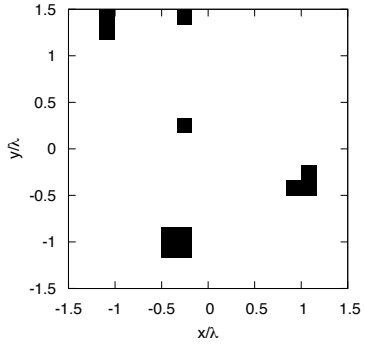
Reconstruction Profiles: $S = 5$ Sparse Cylinders $l = 0.33\lambda$ - Worst Case



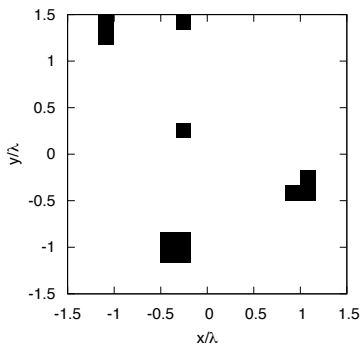
(a)



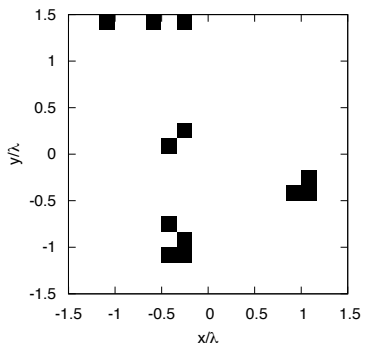
(b)



(c)



(d)



(e)

Figure 28. Actual object (a) and MT-BCS reconstructed object for $SNR = 50$ [dB] (b), $SNR = 30$ [dB] (c), $SNR = 20$ [dB] (d) and $SNR = 10$ [dB] (e).

Resume: Domain $L = 3.0\lambda$ - Statistical Analysis - Error Figures

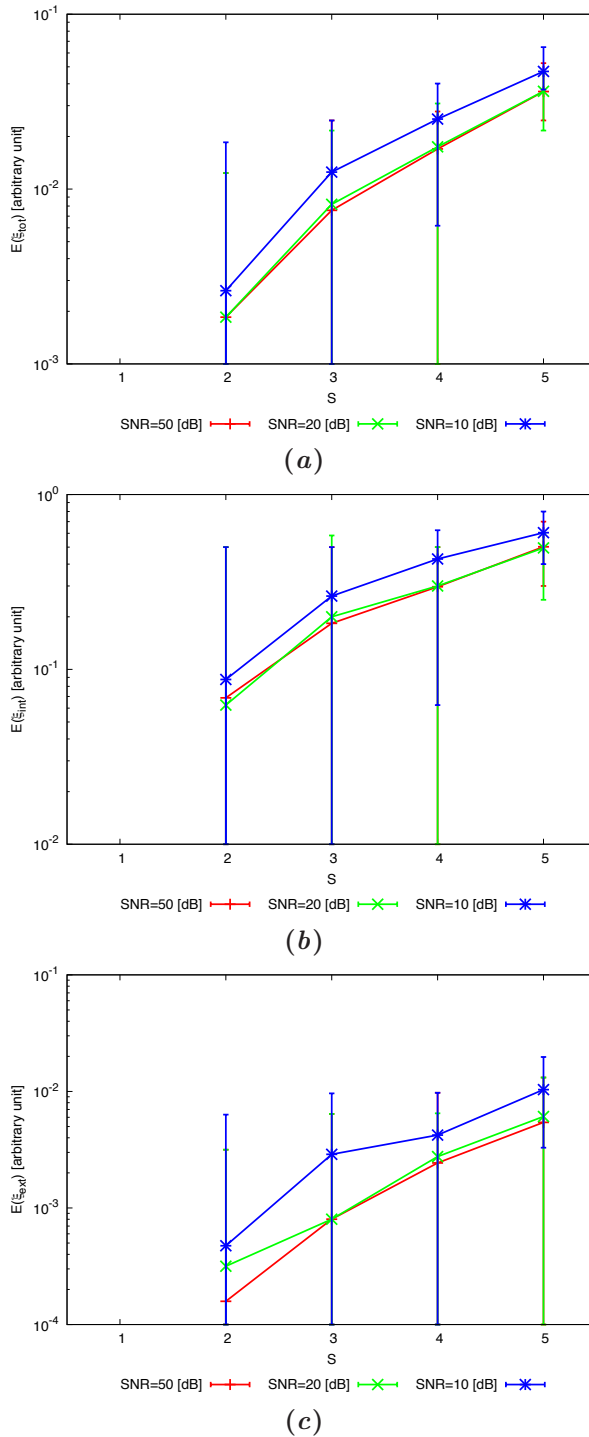


Figure 29. Statistical Analysis - Behavior of mean, maximum and minimum of the error figures as a function of S of the total error ξ_{tot} (a), internal error ξ_{int} (b) and external error ξ_{ext} (c).

3 TESTS Domain $L = 4.00\lambda$

3.1 Tests Random Objects $l = 0.15\lambda$

GOAL: show the performances of *BCS* when dealing with a sparse scatterer

- Number of Views: V
- Number of Measurements: M
- Number of Cells for the Inversion: N
- Number of Cells for the Direct solver: D
- Side of the investigation domain: L

Test Case Description

Direct solver:

- Square domain divided in $\sqrt{D} \times \sqrt{D}$ cells
- Domain side: $L = 3\lambda$
- $D = 1296$ (discretization for the direct solver: $< \lambda/10$)

Investigation domain:

- Square domain divided in $\sqrt{N} \times \sqrt{N}$ cells
- $L = 4\lambda$
- $2ka = 2 \times \frac{2\pi}{\lambda} \times \frac{L\sqrt{2}}{2} = 35.45$
- $\#DOF = \frac{(2ka)^2}{2} = \frac{(2 \times \frac{2\pi}{\lambda} \times \frac{L\sqrt{2}}{2})^2}{2} \approx 648$
- N scelto in modo da essere vicino a $\#DOF$: $N = 676$ (26×26)

Measurement domain:

- Measurement points taken on a circle of radius $\rho = 3\lambda$
- Full-aspect measurements
- $M \approx 2ka \rightarrow M = 36$

Sources:

- Plane waves
- $V \approx 2ka \rightarrow V = 36$
- Amplitude: $A = 1$
- Frequency: 300 MHz ($\lambda = 1$)

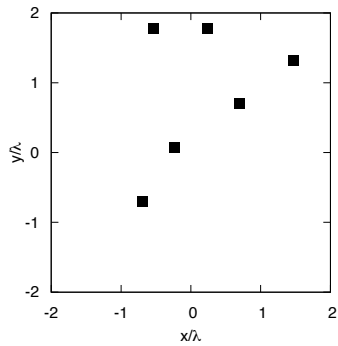
PEC Objects:

- Two square cylinders of side $\frac{2}{13}\lambda \cong 0.15\lambda$
- S sparse square cylinders of side $\frac{2}{13}\lambda \cong 0.15\lambda$ ($S \in \{1, 2, 3, 4, 5, 6, 7, 8, 9, 10, 11, 12\}$). In order to get a statistical validation, for each value of S the simulation has been repeat for 20 times, changing the distribution of the objects inside the investigation domain

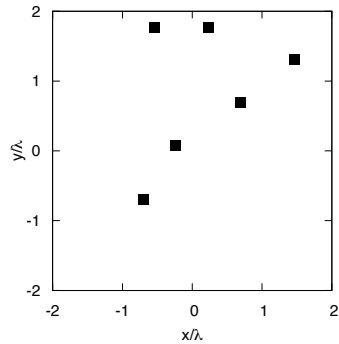
MT-BCS-based technique parameters:

- Gamma prior on noise variance parameter: $a = 5 \times 10^{-2}$
- Gamma prior on noise variance parameter: $b = 5 \times 10^{-2}$
- Convergenze parameter: $\tau = 1.0 \times 10^{-8}$
- Threshold: $\eta = 0.27$

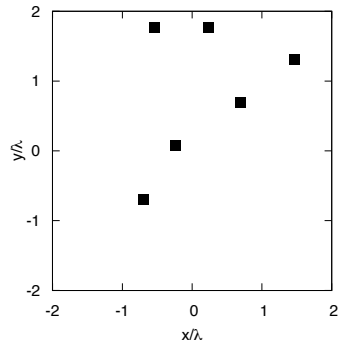
Reconstruction Profiles: $S = 6$ Sparse Cylinders - Best Case



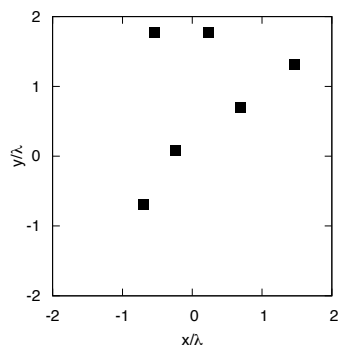
(a)



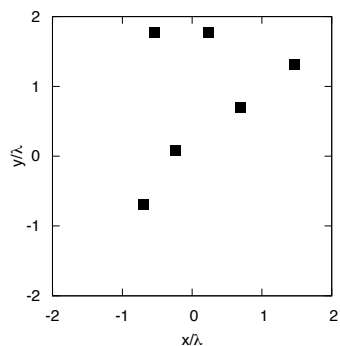
(b)



(c)



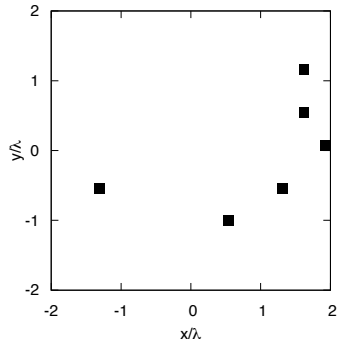
(d)



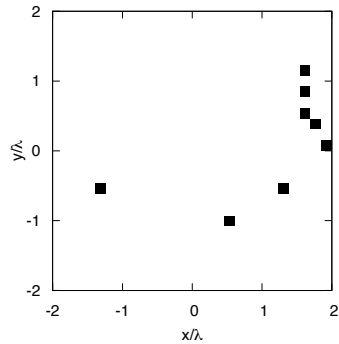
(e)

Figure 30. Actual object (a) and MT-BCS reconstructed object for $SNR = 50$ [dB] (b), $SNR = 30$ [dB] (c), $SNR = 20$ [dB] (d) and $SNR = 10$ [dB] (e).

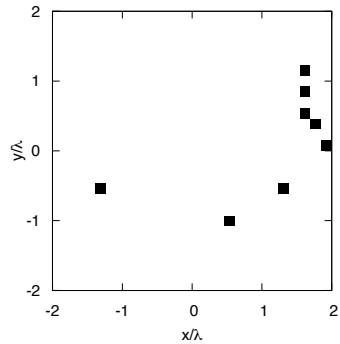
Reconstruction Profiles: $S = 6$ Sparse Cylinders - Worst Case



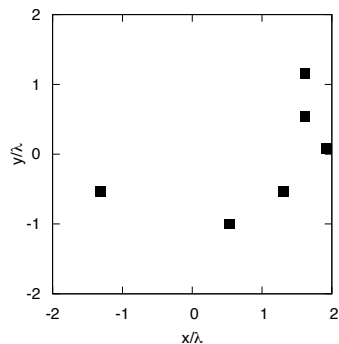
(a)



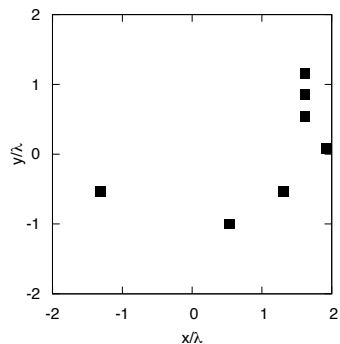
(b)



(c)



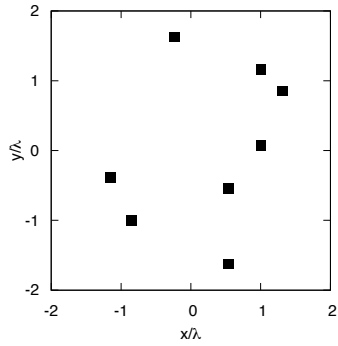
(d)



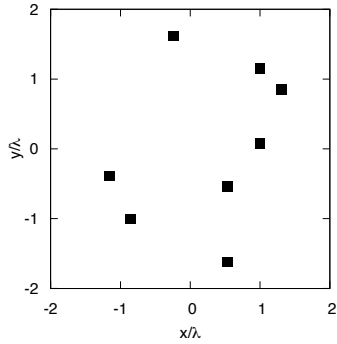
(e)

Figure 31. Actual object (a) and MT-BCS reconstructed object for $SNR = 50$ [dB] (b), $SNR = 30$ [dB] (c), $SNR = 20$ [dB] (d) and $SNR = 10$ [dB] (e).

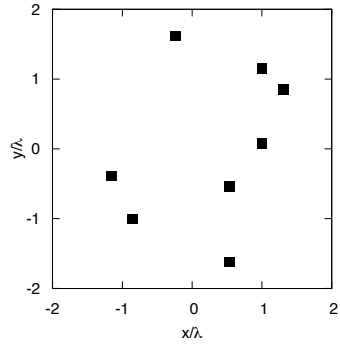
Reconstruction Profiles: $S = 8$ Sparse Cylinders - Best Case



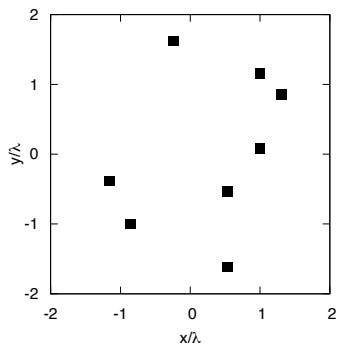
(a)



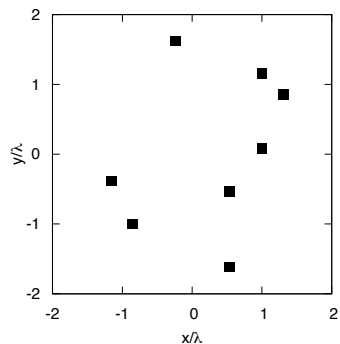
(b)



(c)



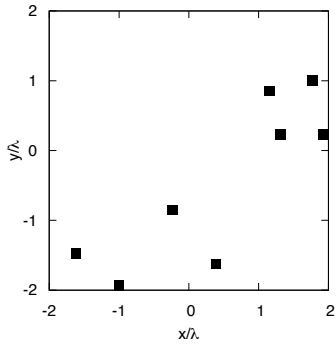
(d)



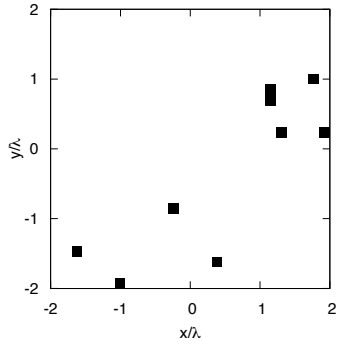
(e)

Figure 32. Actual object (a) and MT-BCS reconstructed object for $SNR = 50$ [dB] (b), $SNR = 30$ [dB] (c), $SNR = 20$ [dB] (d) and $SNR = 10$ [dB] (e).

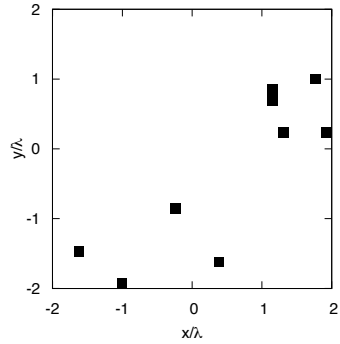
Reconstruction Profiles: $S = 8$ Sparse Cylinders - Worst Case



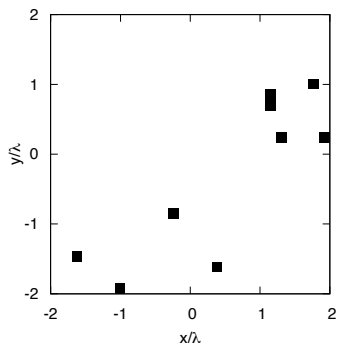
(a)



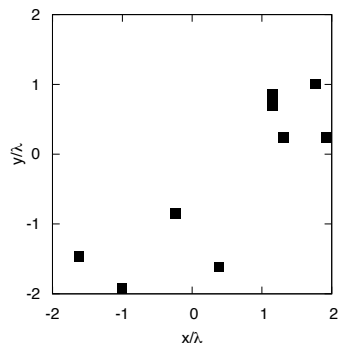
(b)



(c)



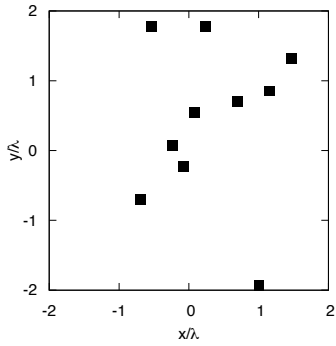
(d)



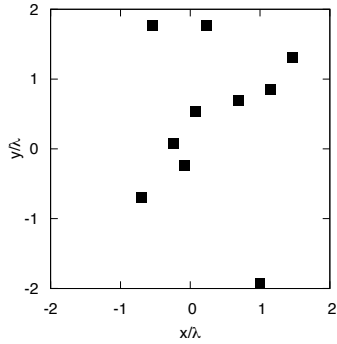
(e)

Figure 33. Actual object (a) and MT-BCS reconstructed object for $SNR = 50$ [dB] (b), $SNR = 30$ [dB] (c), $SNR = 20$ [dB] (d) and $SNR = 10$ [dB] (e).

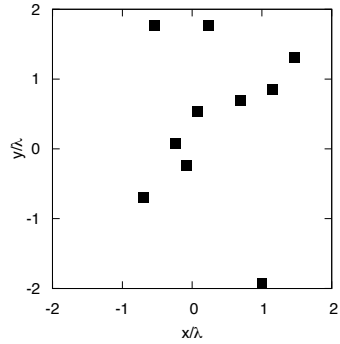
Reconstruction Profiles: $S = 10$ Sparse Cylinders - Best Case



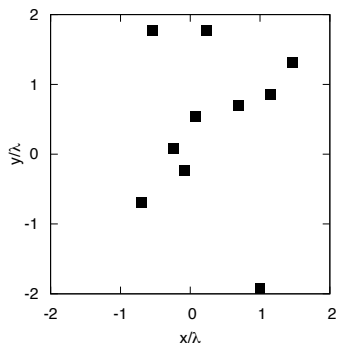
(a)



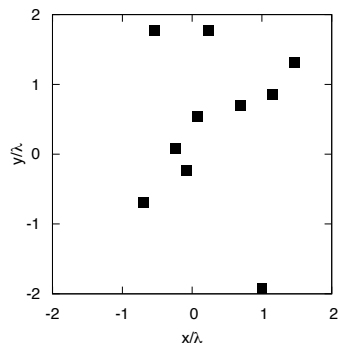
(b)



(c)



(d)



(e)

Figure 34. Actual object (a) and MT-BCS reconstructed object for $SNR = 50$ [dB] (b), $SNR = 30$ [dB] (c), $SNR = 20$ [dB] (d) and $SNR = 10$ [dB] (e).

Reconstruction Profiles: $S = 10$ Sparse Cylinders - Worst Case

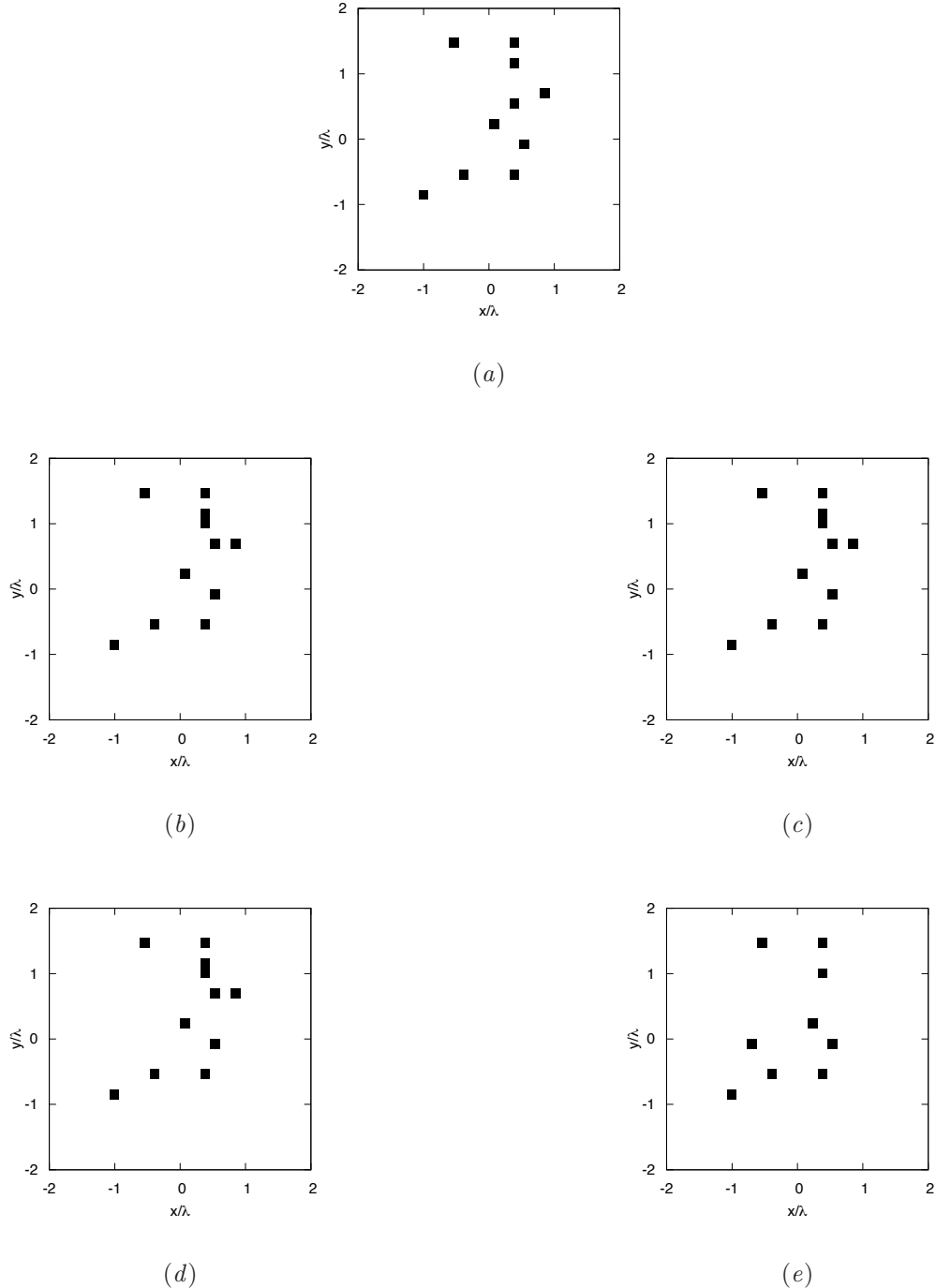
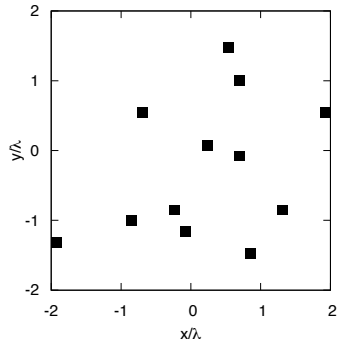
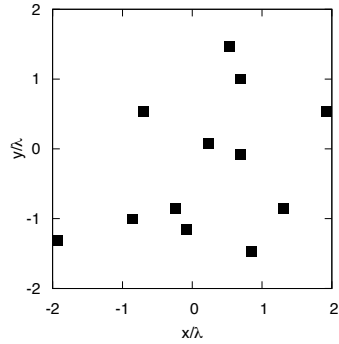


Figure 35. Actual object (a) and MT-BCS reconstructed object for $SNR = 50$ [dB] (b), $SNR = 30$ [dB] (c), $SNR = 20$ [dB] (d) and $SNR = 10$ [dB] (e).

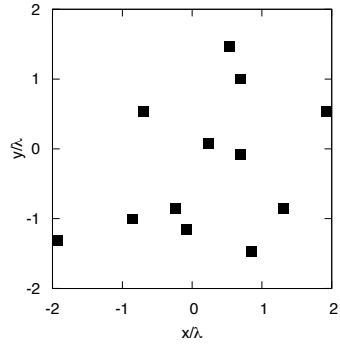
Reconstruction Profiles: $S = 12$ Sparse Cylinders - Best Case



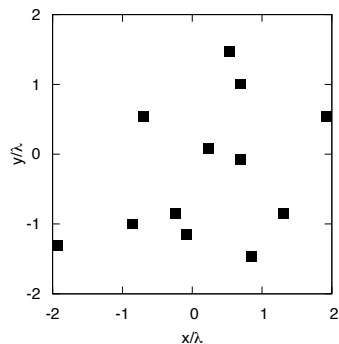
(a)



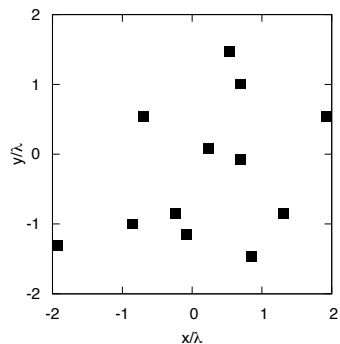
(b)



(c)



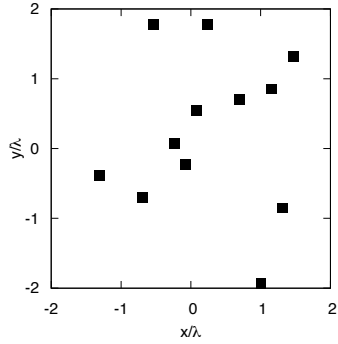
(d)



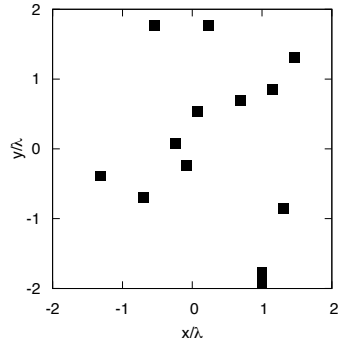
(e)

Figure 36. Actual object (a) and MT-BCS reconstructed object for $SNR = 50$ [dB] (b), $SNR = 30$ [dB] (c), $SNR = 20$ [dB] (d) and $SNR = 10$ [dB] (e).

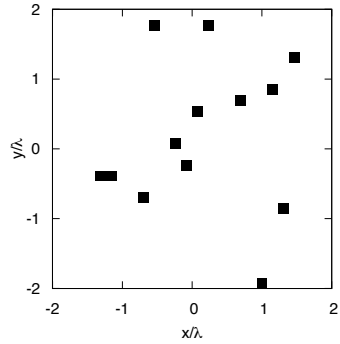
Reconstruction Profiles: $S = 12$ Sparse Cylinders - Worst Case



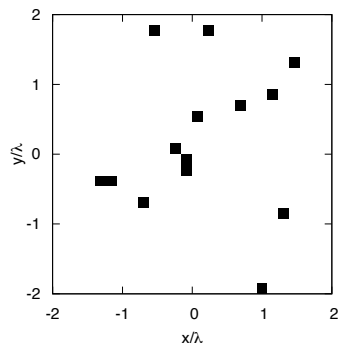
(a)



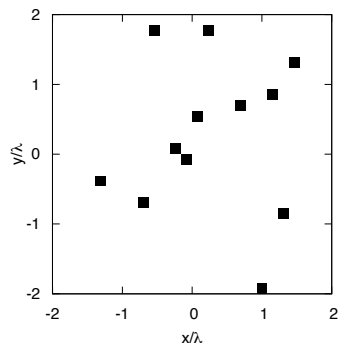
(b)



(c)



(d)



(e)

Figure 37. Actual object (a) and MT-BCS reconstructed object for $SNR = 50$ [dB] (b), $SNR = 30$ [dB] (c), $SNR = 20$ [dB] (d) and $SNR = 10$ [dB] (e).

Resume: Domain $L = 4.0\lambda$ - Statistical Analysis - Error Figures

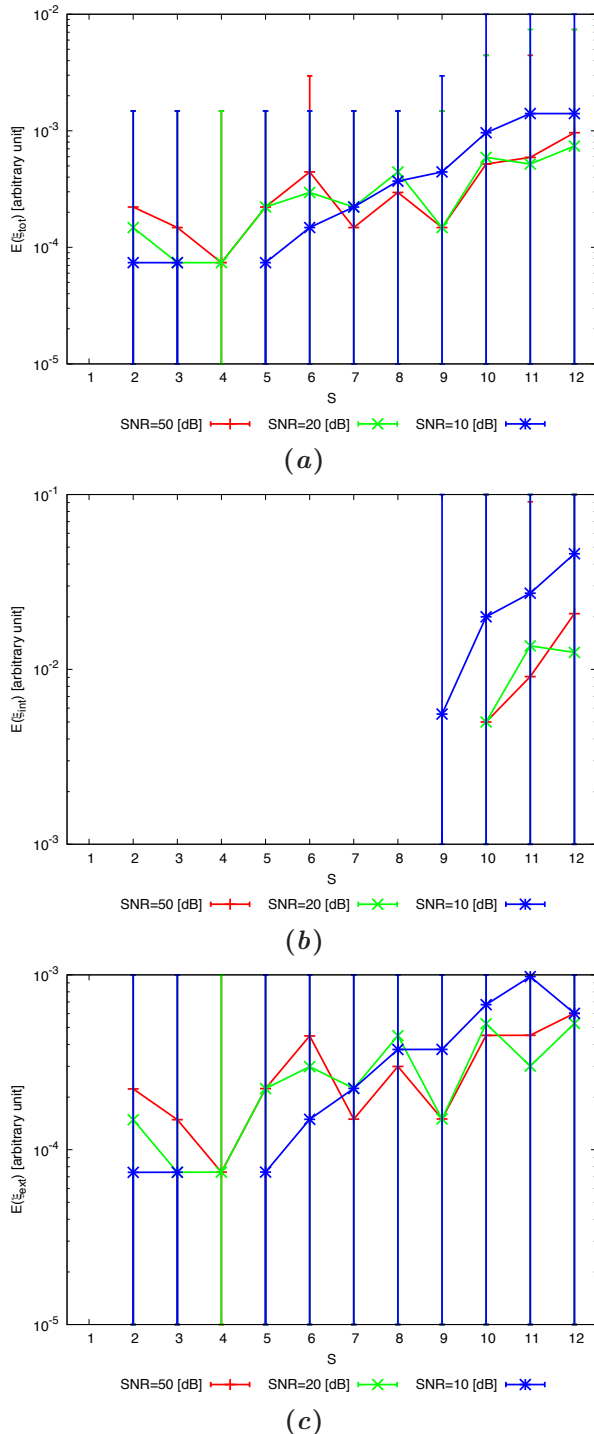


Figure 38. Statistical Analysis - Behavior of mean, maximum and minimum of the error figures as a function of S of the total error ξ_{tot} (a), internal error ξ_{int} (b) and external error ξ_{ext} (c).

4 TESTS Domain $L = 5.00\lambda$

4.1 Tests Random Objects $l = 0.15\lambda$

GOAL: show the performances of *BCS* when dealing with a sparse scatterer

- Number of Views: V
- Number of Measurements: M
- Number of Cells for the Inversion: N
- Number of Cells for the Direct solver: D
- Side of the investigation domain: L

Test Case Description

Direct solver:

- Square domain divided in $\sqrt{D} \times \sqrt{D}$ cells
- Domain side: $L = 3\lambda$
- $D = 4096$ (discretization for the direct solver: $< \lambda/10$)

Investigation domain:

- Square domain divided in $\sqrt{N} \times \sqrt{N}$ cells
- $L = 4\lambda$
- $2ka = 2 \times \frac{2\pi}{\lambda} \times \frac{L\sqrt{2}}{2} = 44.43$
- $\#DOF = \frac{(2ka)^2}{2} = \frac{(2 \times \frac{2\pi}{\lambda} \times \frac{L\sqrt{2}}{2})^2}{2} \approx 1012.3$
- N scelto in modo da essere vicino a $\#DOF$: $N = 1024$ (32×32)

Measurement domain:

- Measurement points taken on a circle of radius $\rho = 5\lambda$
- Full-aspect measurements
- $M \approx 2ka \rightarrow M = 45$

Sources:

- Plane waves
- $V \approx 2ka \rightarrow V = 45$
- Amplitude: $A = 1$
- Frequency: 300 MHz ($\lambda = 1$)

PEC Objects:

- Two square cylinders of side $\frac{5}{32}\lambda \cong 0.16\lambda$
- S sparse square cylinders of side $\frac{5}{32}\lambda \cong 0.16\lambda$ ($S \in \{2, 4, 6, 8, 10, 12, 14, 16, 18, 20\}$). In order to get a statistical validation, for each value of S the simulation has been repeat for 20 times, changing the distribution of the objects inside the investigation domain

MT-BCS-based technique parameters:

- Gamma prior on noise variance parameter: $a = 5 \times 10^{-2}$
- Gamma prior on noise variance parameter: $b = 5 \times 10^{-2}$
- Convergenze parameter: $\tau = 1.0 \times 10^{-8}$
- Threshold: $\eta = 0.27$

Reconstruction Profiles: $S = 10$ Sparse Cylinders - Best Case

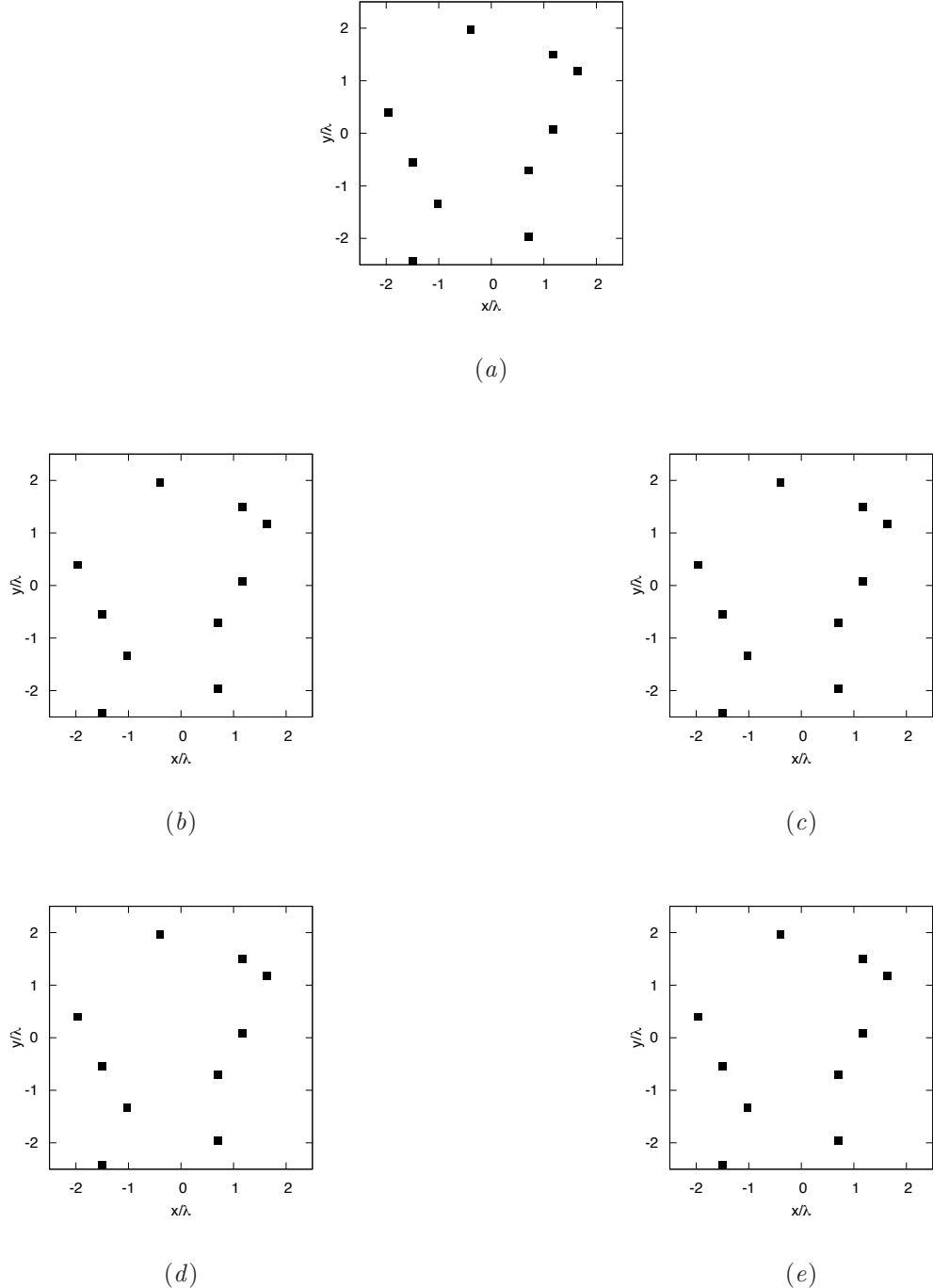
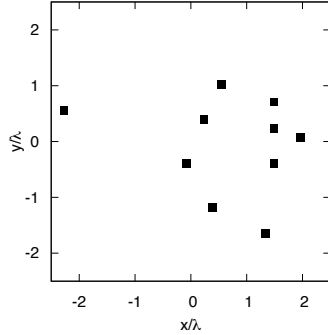
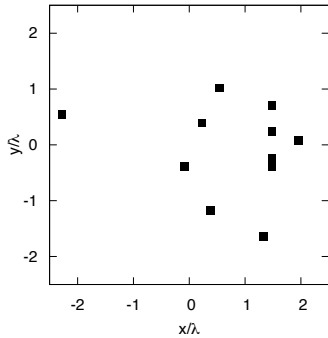


Figure 39. Actual object (a) and MT-BCS reconstructed object for $SNR = 50$ [dB] (b), $SNR = 30$ [dB] (c), $SNR = 20$ [dB] (d) and $SNR = 10$ [dB] (e).

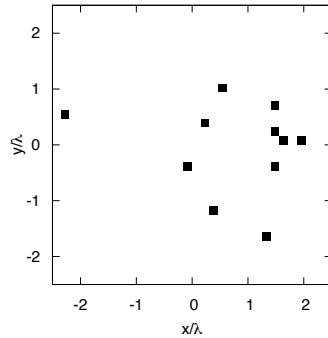
Reconstruction Profiles: $S = 10$ Sparse Cylinders - Worst Case



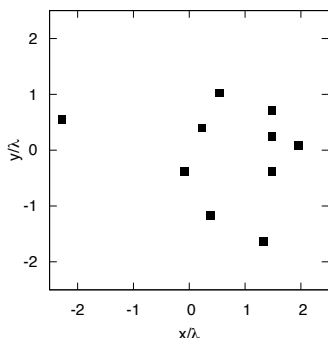
(a)



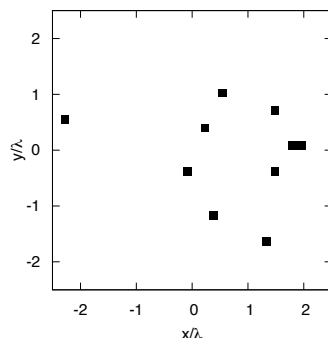
(b)



(c)



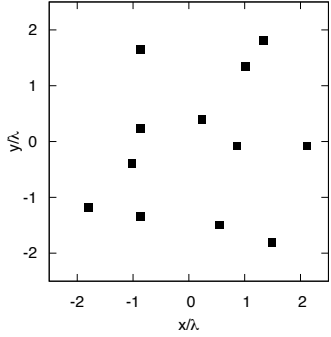
(d)



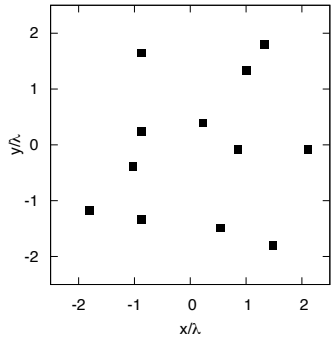
(e)

Figure 40. Actual object (a) and MT-BCS reconstructed object for $SNR = 50$ [dB] (b), $SNR = 30$ [dB] (c), $SNR = 20$ [dB] (d) and $SNR = 10$ [dB] (e).

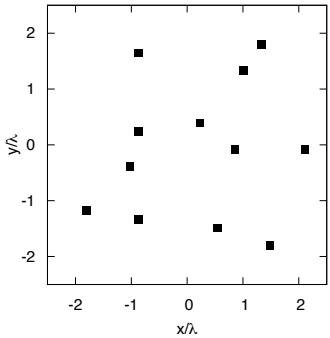
Reconstruction Profiles: $S = 12$ Sparse Cylinders - Best Case



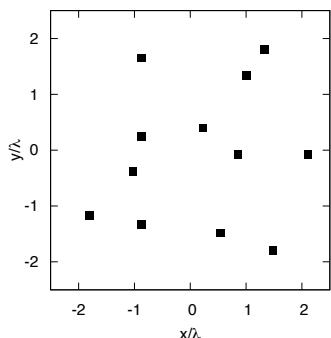
(a)



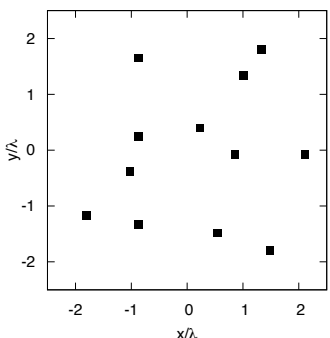
(b)



(c)



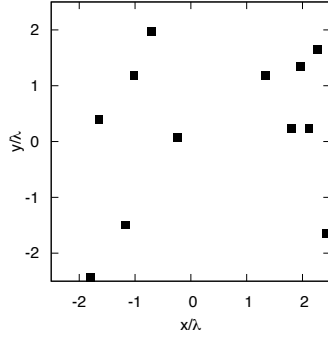
(d)



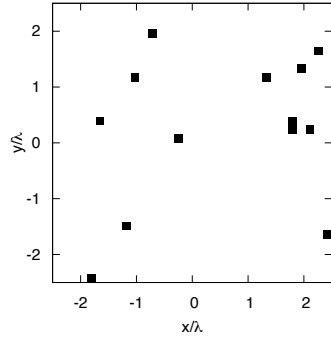
(e)

Figure 41. Actual object (a) and MT-BCS reconstructed object for $SNR = 50$ [dB] (b), $SNR = 30$ [dB] (c), $SNR = 20$ [dB] (d) and $SNR = 10$ [dB] (e).

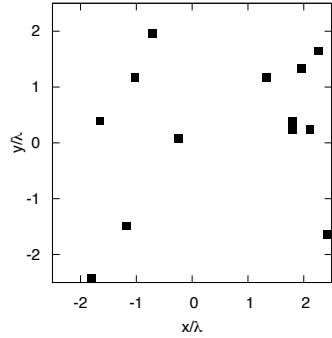
Reconstruction Profiles: $S = 12$ Sparse Cylinders - Worst Case



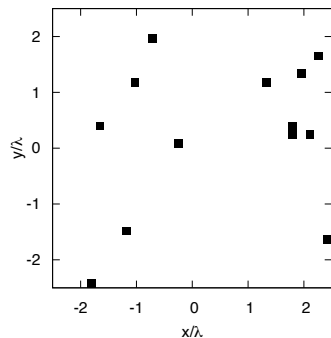
(a)



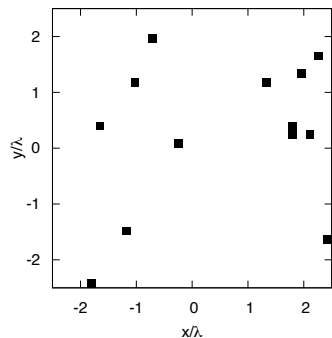
(b)



(c)



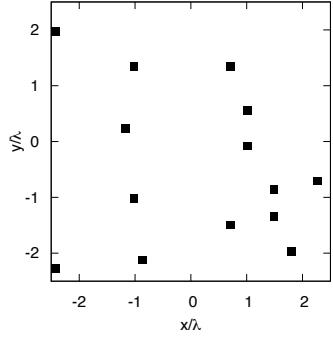
(d)



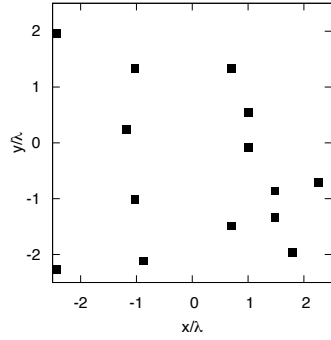
(e)

Figure 42. Actual object (a) and MT-BCS reconstructed object for $SNR = 50$ [dB] (b), $SNR = 30$ [dB] (c), $SNR = 20$ [dB] (d) and $SNR = 10$ [dB] (e).

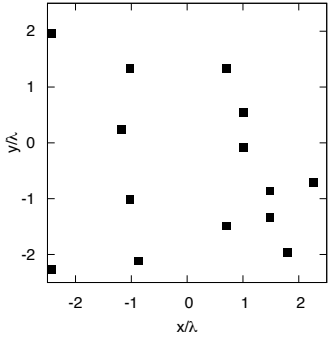
Reconstruction Profiles: $S = 14$ Sparse Cylinders - Best Case



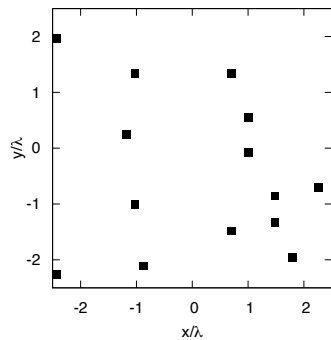
(a)



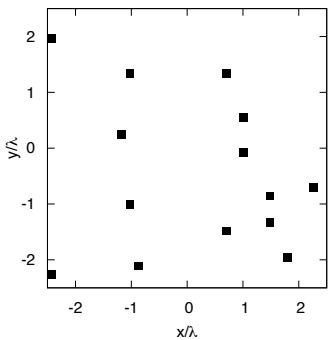
(b)



(c)



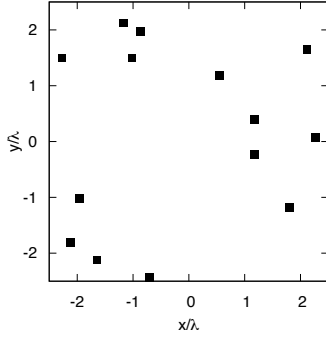
(d)



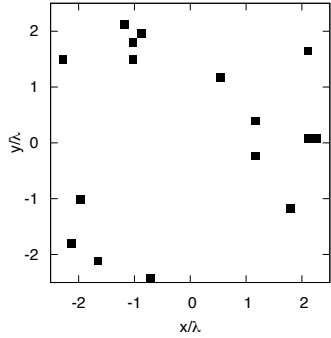
(e)

Figure 43. Actual object (a) and MT-BCS reconstructed object for $SNR = 50$ [dB] (b), $SNR = 30$ [dB] (c), $SNR = 20$ [dB] (d) and $SNR = 10$ [dB] (e).

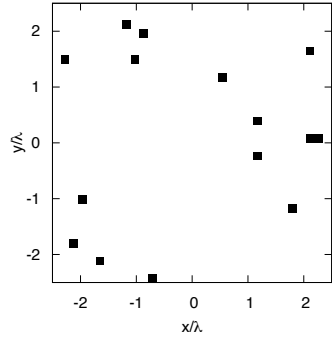
Reconstruction Profiles: $S = 14$ Sparse Cylinders - Worst Case



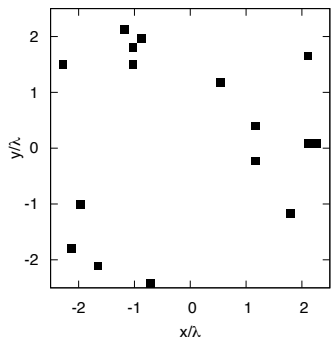
(a)



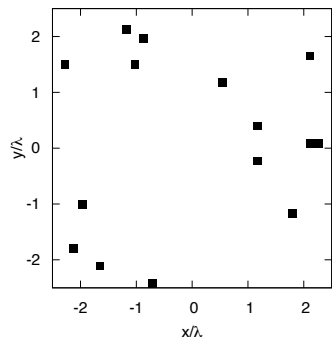
(b)



(c)



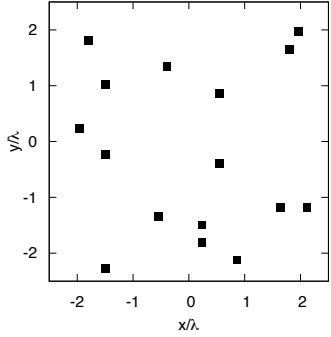
(d)



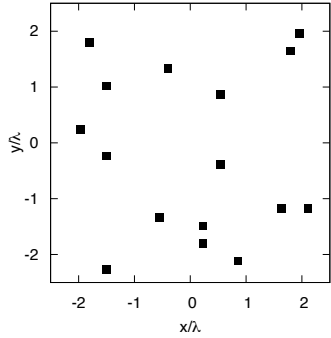
(e)

Figure 44. Actual object (a) and MT-BCS reconstructed object for $SNR = 50$ [dB] (b), $SNR = 30$ [dB] (c), $SNR = 20$ [dB] (d) and $SNR = 10$ [dB] (e).

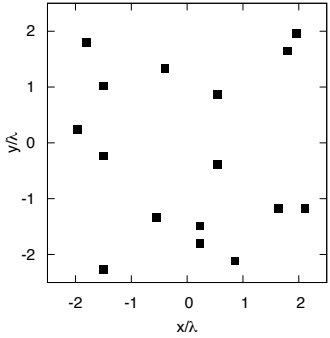
Reconstruction Profiles: $S = 16$ Sparse Cylinders - Best Case



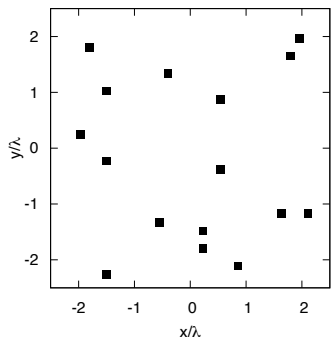
(a)



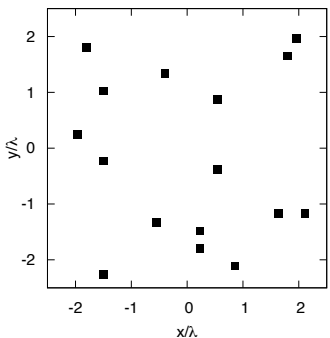
(b)



(c)



(d)



(e)

Figure 45. Actual object (a) and MT-BCS reconstructed object for $SNR = 50$ [dB] (b), $SNR = 30$ [dB] (c), $SNR = 20$ [dB] (d) and $SNR = 10$ [dB] (e).

Reconstruction Profiles: $S = 16$ Sparse Cylinders - Worst Case

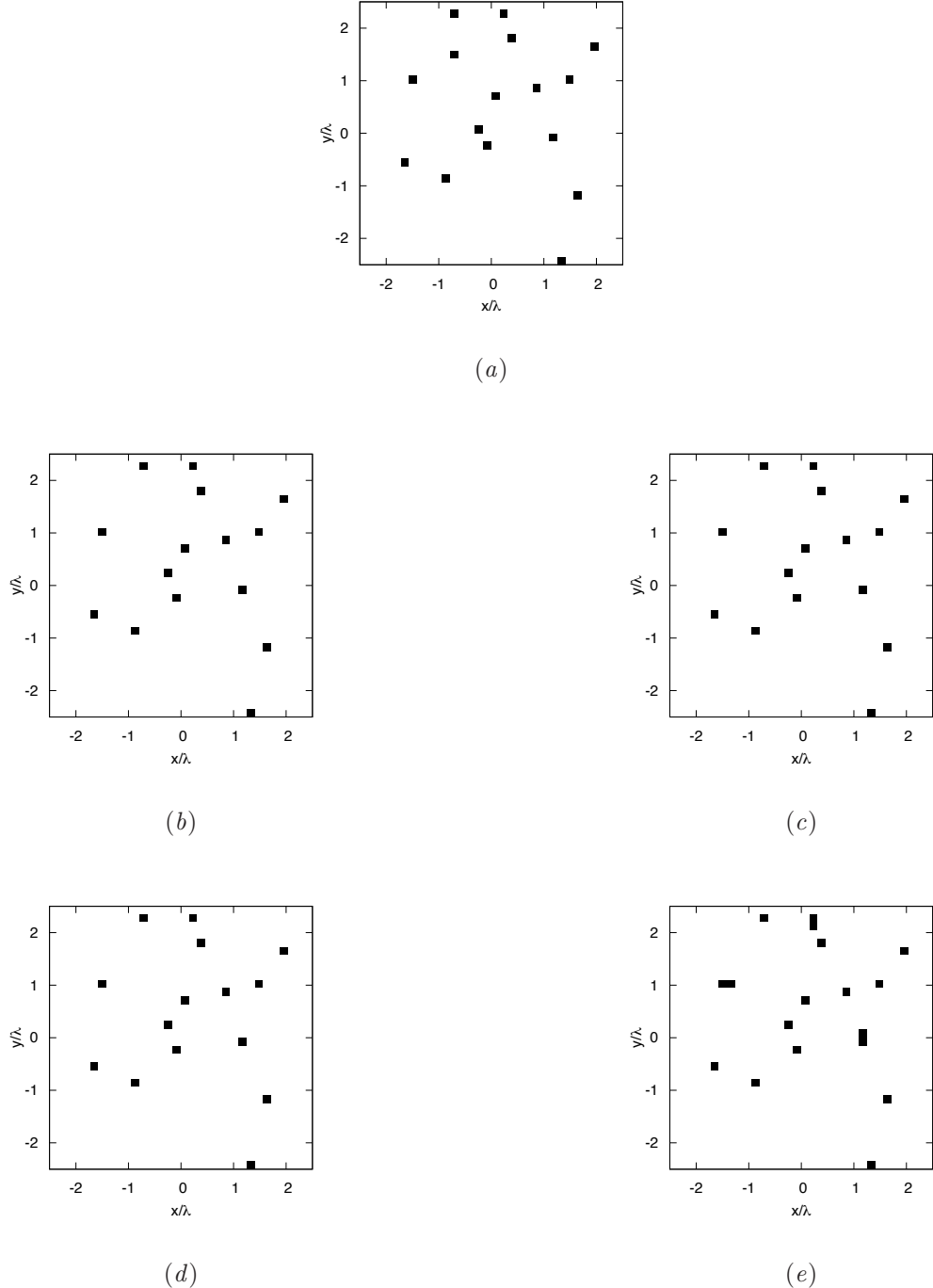


Figure 46. Actual object (a) and MT-BCS reconstructed object for $SNR = 50$ [dB] (b), $SNR = 30$ [dB] (c), $SNR = 20$ [dB] (d) and $SNR = 10$ [dB] (e).

Reconstruction Profiles: $S = 18$ Sparse Cylinders - Best Case

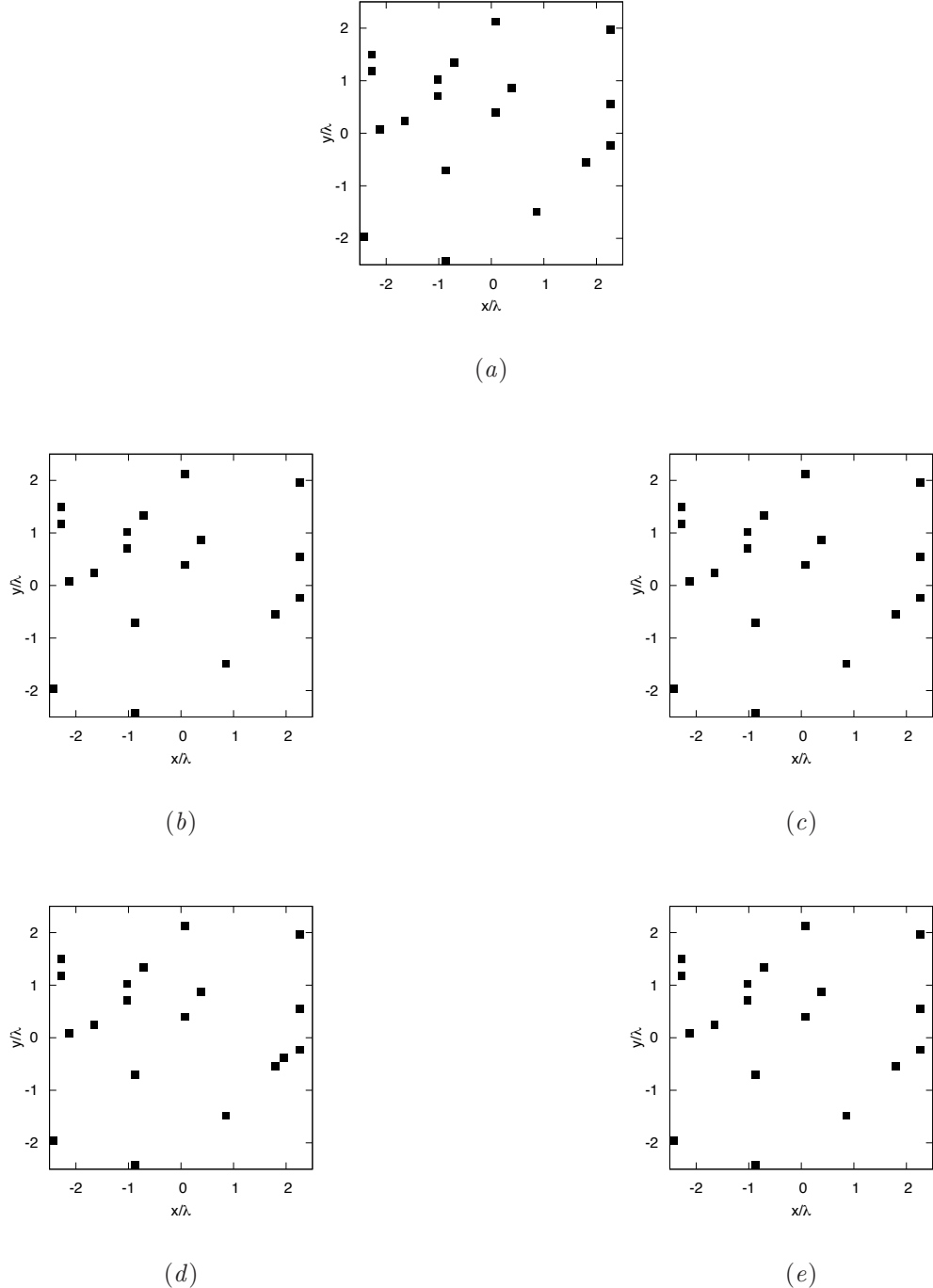
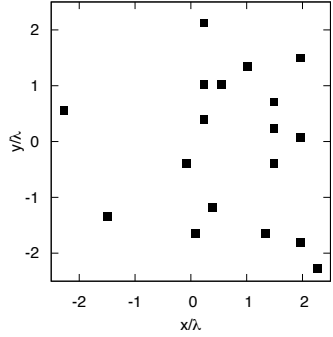
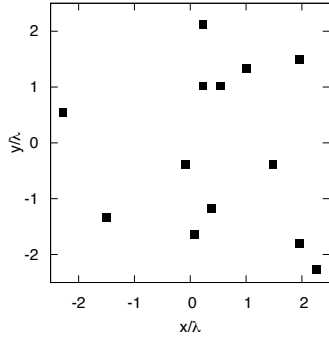


Figure 47. Actual object (a) and MT-BCS reconstructed object for $SNR = 50$ [dB] (b), $SNR = 30$ [dB] (c), $SNR = 20$ [dB] (d) and $SNR = 10$ [dB] (e).

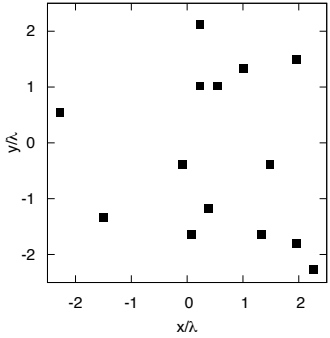
Reconstruction Profiles: $S = 18$ Sparse Cylinders - Worst Case



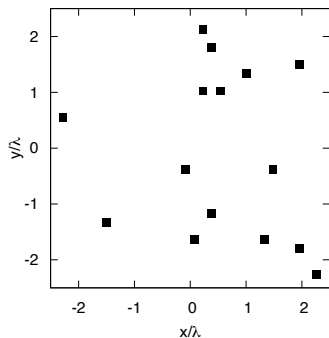
(a)



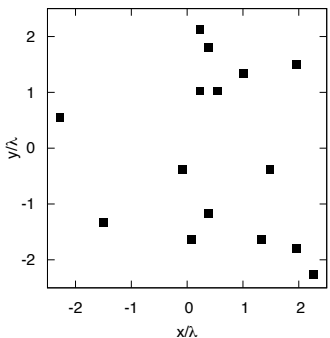
(b)



(c)



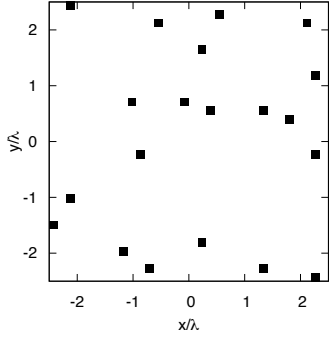
(d)



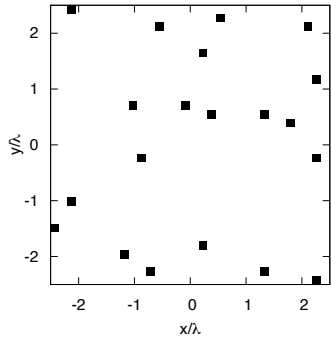
(e)

Figure 48. Actual object (a) and MT-BCS reconstructed object for $SNR = 50$ [dB] (b), $SNR = 30$ [dB] (c), $SNR = 20$ [dB] (d) and $SNR = 10$ [dB] (e).

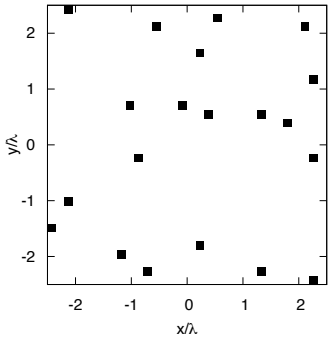
Reconstruction Profiles: $S = 20$ Sparse Cylinders - Best Case



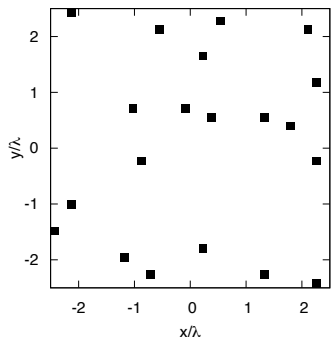
(a)



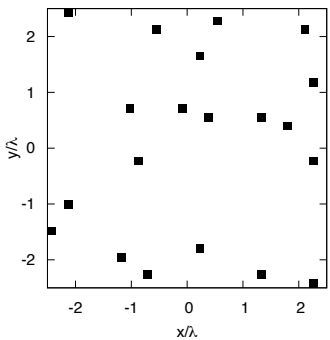
(b)



(c)



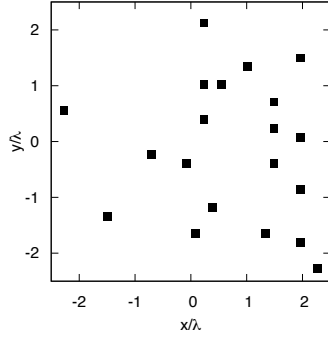
(d)



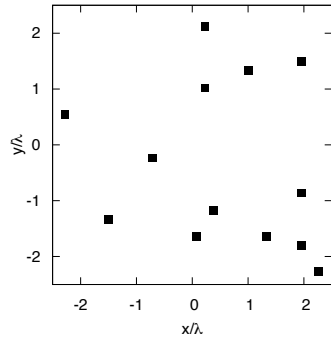
(e)

Figure 49. Actual object (a) and MT-BCS reconstructed object for $SNR = 50$ [dB] (b), $SNR = 30$ [dB] (c), $SNR = 20$ [dB] (d) and $SNR = 10$ [dB] (e).

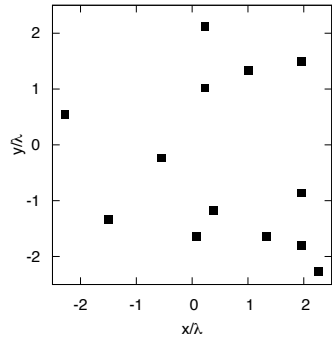
Reconstruction Profiles: $S = 20$ Sparse Cylinders - Worst Case



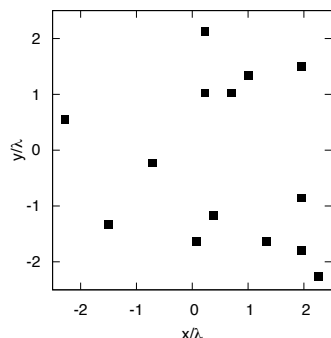
(a)



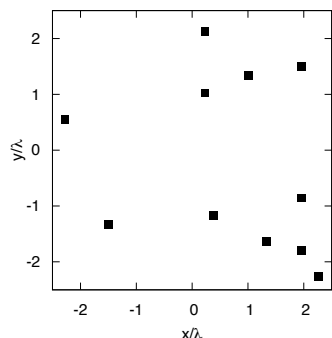
(b)



(c)



(d)



(e)

Figure 50. Actual object (a) and MT-BCS reconstructed object for $SNR = 50$ [dB] (b), $SNR = 30$ [dB] (c), $SNR = 20$ [dB] (d) and $SNR = 10$ [dB] (e).

Resume: Domain $L = 5.0\lambda$ - Statistical Analysis - Error Figures

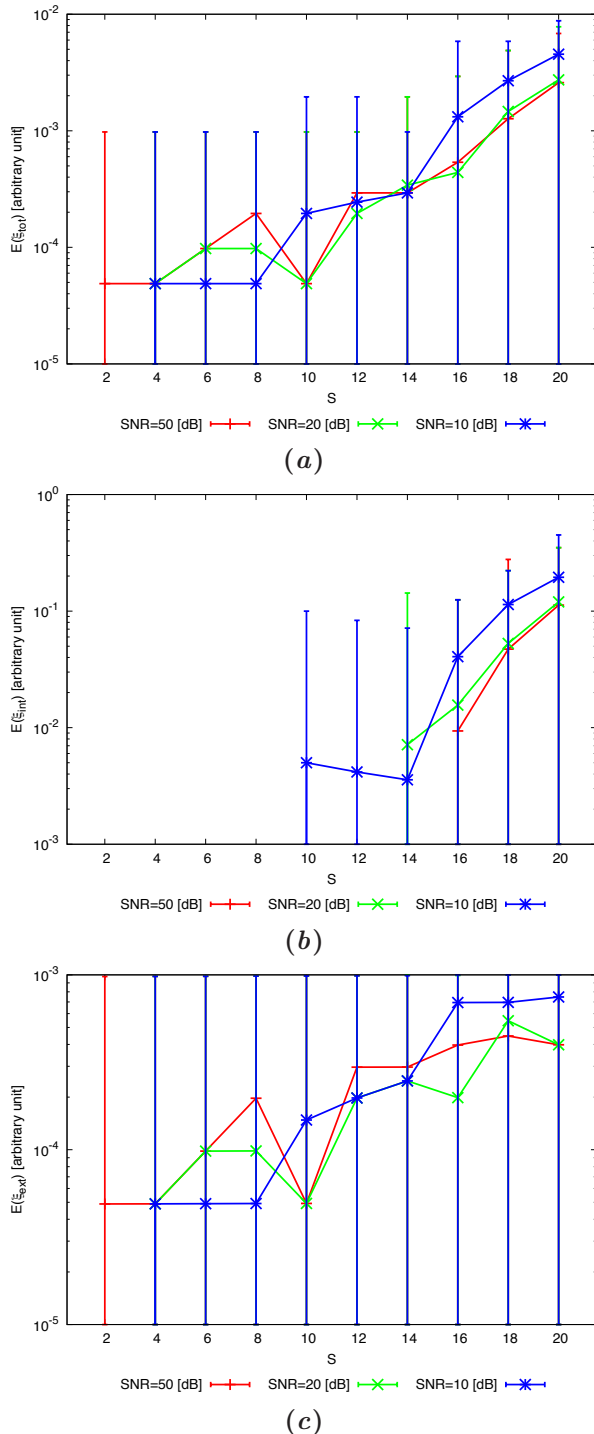


Figure 51. Statistical Analysis - Behavior of mean, maximum and minimum of the error figures as a function of S of the total error ξ_{tot} (a), internal error ξ_{int} (b) and external error ξ_{ext} (c).

References

- [1] L. Poli, G. Oliveri, and A. Massa, "Imaging sparse metallic cylinders through a Local Shape Function Bayesian Compressive Sensing approach," *Journal of Optical Society of America A*, vol. 30, no. 6, pp. 1261-1272, 2013.
- [2] F. Viani, L. Poli, G. Oliveri, F. Robol, and A. Massa, "Sparse scatterers imaging through approximated multitask compressive sensing strategies," *Microwave Opt. Technol. Lett.*, vol. 55, no. 7, pp. 1553-1558, Jul. 2013.
- [3] L. Poli, G. Oliveri, P. Rocca, and A. Massa, "Bayesian compressive sensing approaches for the reconstruction of two-dimensional sparse scatterers under TE illumination," *IEEE Trans. Geosci. Remote Sensing*, vol. 51, no. 5, pp. 2920-2936, May. 2013.
- [4] L. Poli, G. Oliveri, and A. Massa, "Microwave imaging within the first-order Born approximation by means of the contrast-field Bayesian compressive sensing," *IEEE Trans. Antennas Propag.*, vol. 60, no. 6, pp. 2865-2879, Jun. 2012.
- [5] G. Oliveri, P. Rocca, and A. Massa, "A bayesian compressive sampling-based inversion for imaging sparse scatterers," *IEEE Trans. Geosci. Remote Sensing*, vol. 49, no. 10, pp. 3993-4006, Oct. 2011.
- [6] G. Oliveri, L. Poli, P. Rocca, and A. Massa, "Bayesian compressive optical imaging within the Rytov approximation," *Optics Letters*, vol. 37, no. 10, pp. 1760-1762, 2012.
- [7] L. Poli, G. Oliveri, F. Viani, and A. Massa, "MT-BCS-based microwave imaging approach through minimum-norm current expansion," *IEEE Trans. Antennas Propag.*, vol. 61, no. 9, pp. 4722-4732, Sept. 2013.
- [8] G. Oliveri, N. Anselmi, and A. Massa, "Compressive sensing imaging of non-sparse 2D scatterers by a total-variation approach within the Born approximation," *IEEE Trans. Antennas Propag.*, 2014, submitted.
- [9] G. Oliveri, A. Randazzo, M. Pastorino, and A. Massa, "Electromagnetic imaging within the contrast-source formulation by means of the multiscaling inexact Newton method," *Journal of Optical Society of America A*, vol. 29, no. 6, pp. 945-958, 2012.
- [10] M. Benedetti, D. Lesselier, M. Lambert, and A. Massa, "Multiple shapes reconstruction by means of multi-region level sets," *IEEE Trans. Geosci. Remote Sensing*, vol. 48, no. 5, pp. 2330-2342, May 2010.
- [11] M. Benedetti, D. Lesselier, M. Lambert, and A. Massa, "A multi-resolution technique based on shape optimization for the reconstruction of homogeneous dielectric objects," *Inverse Problems*, vol. 25, no. 1, pp. 1-26, Jan. 2009.
- [12] M. Salucci, D. Sartori, N. Anselmi, A. Randazzo, G. Oliveri, and A. Massa, "Imaging buried objects within the second-order Born approximation through a multiresolution-regularized inexact-Newton method", in 2013 International Symposium on Electromagnetic Theory (EMTS), Hiroshima, Japan, pp. 116-118, May 20-24, 2013.